GLOBAL CLIMATE BULLETIN
n°198 – December 2015

Table of Contents

I. DESCRIPTION OF THE CLIMATE SYSTEM (October 2015) 2
I.1. Oceanic analysis 2
I.1.a Global analysis 2
I.1.b Near Europe 5
I.2. Atmosphère 6
I.2.a General Circulation 6
I.2.b Precipitation 11
I.2.c Temperature 14
I.2.d Sea ice 16
II. SEASONAL FORECAST FROM DYNAMICAL MODELS 17
II.1. OCEANIC FORECASTS 17
II.1.a Sea surface temperature (SST) 17
II.1.b ENSO forecast 20
II.1.c Atlantic ocean forecasts 21
II.1.d Indian ocean forecasts 21
II.2. GENERAL CIRCULATION FORECAST 23
II.2.a Global forecast 23
II.2.b North hemisphere forecast and Europe 25
II.3. IMPACT: TEMPERATURE FORECASTS 26
II.3.a ECMWF 27
II.3.b Météo-France 27
II.3.c Japan Meteorological Agency (JMA) 28
II.3.d EUROSIP 28
II.4. IMPACT : PRECIPITATION FORECAST 29
II.4.a ECMWF 29
II.4.b Météo-France 30
II.4.c Japan Meteorological Agency (JMA) 31
II.4.d EUROSIP 32
II.5. REGIONAL TEMPERATURES and PRECIPITATIONS 33
II.6. MODEL'S CONSISTENCY 34
II.7. "EXTREME" SCENARIOS 34
II.8. DISCUSSION AND SUMMARY 35
II.8.a Forecast over Europe 35
II.8.b Tropical cyclone activity 37
II.9. Seasonal Forecasts 38
II.10. « NINO », SOI indices and Oceanic boxes 38
II.11. Land Boxes 39
II.12. Acknowledgement 39

I. DESCRIPTION OF THE CLIMATE SYSTEM (OCTOBER 2015)

I.1. OCEANIC ANALYSIS

I.1.a Global analysis

In the Pacific ocean :

All along the equatorial waveguide :

- Surface (fig.I.1.1, I.1.2 and I.1.3): The strong El Nino event is now well installed. Strong warm anomaly along the equator from the International Date Line to the South American coasts. The SST anomaly has reinforced in October in the central part of the basin. In October, the Nino3.4 index value monthly mean reaches +2.5°C, and the Nino1+2 index 2.5 ° C.

- Sub-surface : remaining East-West dipole anomaly pattern. Kevin wave visible between mid-September and mid-October.

El Niño monitoring: Niño 3.4 index reaches 2.5 °C in October (monthly mean), corresponding to a strong El Niño event.

Elsewhere:

In the northern hemisphere: still a clear positive structure of the PDO. The anomalies are particularly strong and little change between Hawaii and California.

In the southern hemisphere: strengthening cold anomaly pattern over Indonesia and along the SPCZ.

In the Indian Ocean :

Generalized warm anomaly, stronger along the African coast and Arabian Sea, and since October close to Australia. The DMI index is still positive around +1°C (http://now notably positive, see for instance stateoftheocean.osmc.noaa.gov/sur/ind/dmi.php)

In the Atlantic:

Close to neutral on the equator and up to 30S.

In the north intertropical aera and along the US coasts, persistant warm anomaly.

In the North Atlantic, the strong cold anomaly from Labrador to Europe is enlarging in its Southern part.

The Mediterranean Sea is still warmer than normal, despite a significant decreasing anomaly in its Northern part in October.

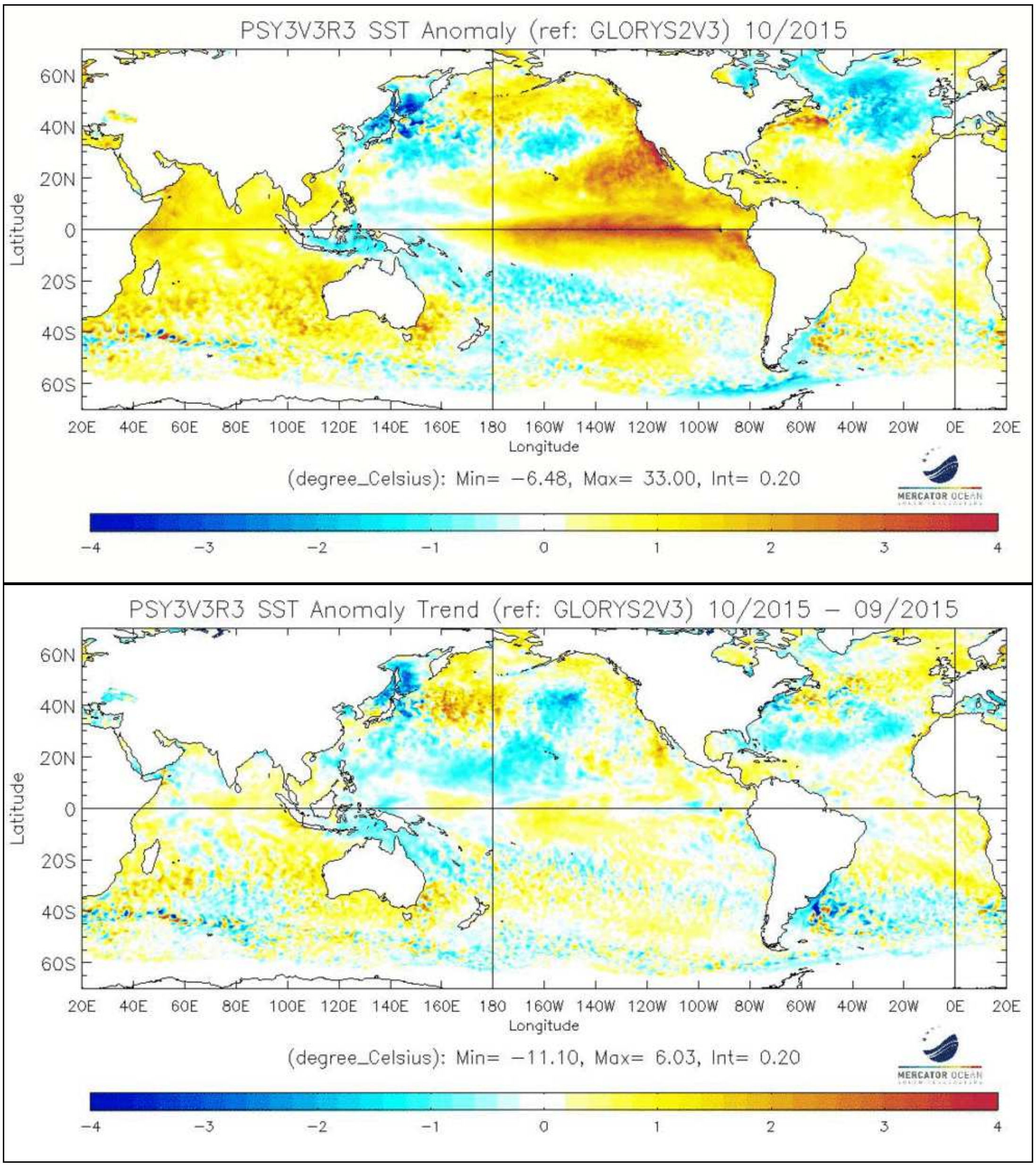

fig.I.1.1: top : SSTs Anomalies (°C) . Bottom : SST tendency (current – previous month), (reference Glorys 1992-2009). http://bcg.mercator-ocean.fr/

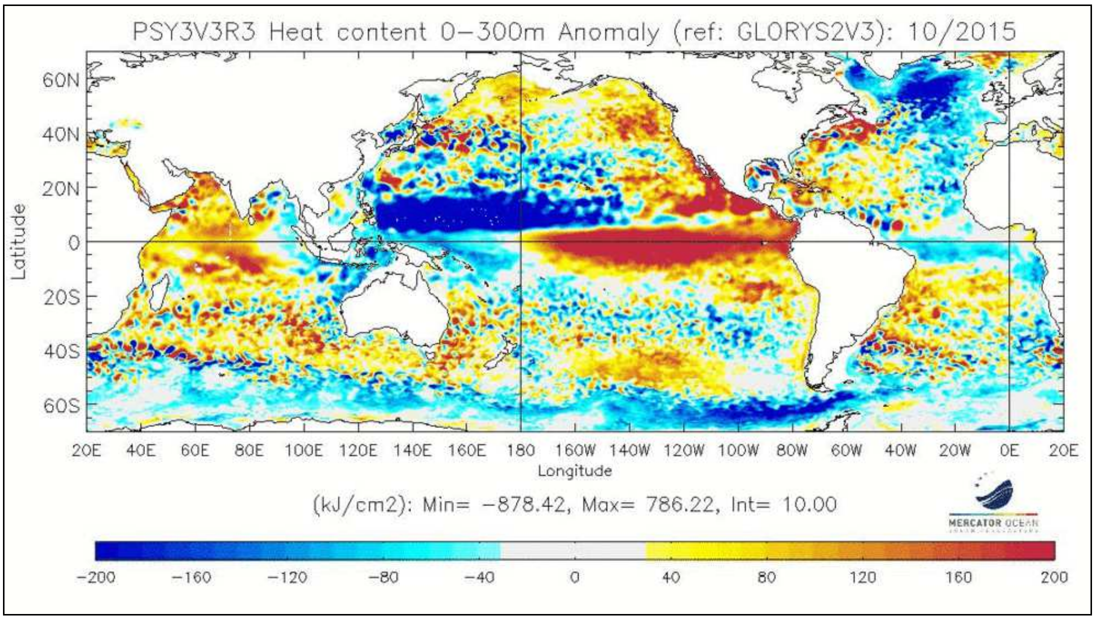

fig.I.1.2: map of Heat Content Anomalies (first 300m, kJ/cm2, reference Glorys 1992-2009)

http://bcg.mercator-ocean.fr/

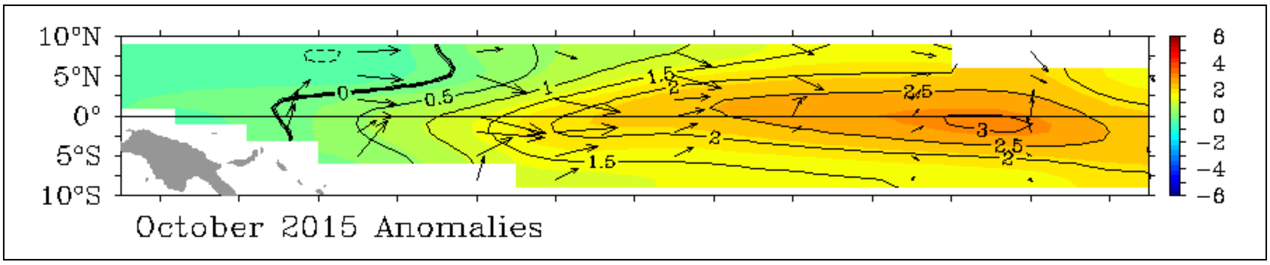

fig.I.1.3: SST Anomalies and Wind anomalies over the Equatorial Pacific from TAO/TRITON.

http://www.pmel.noaa.gov/tao/jsdisplay/monthly-summary/monthly-summary.html

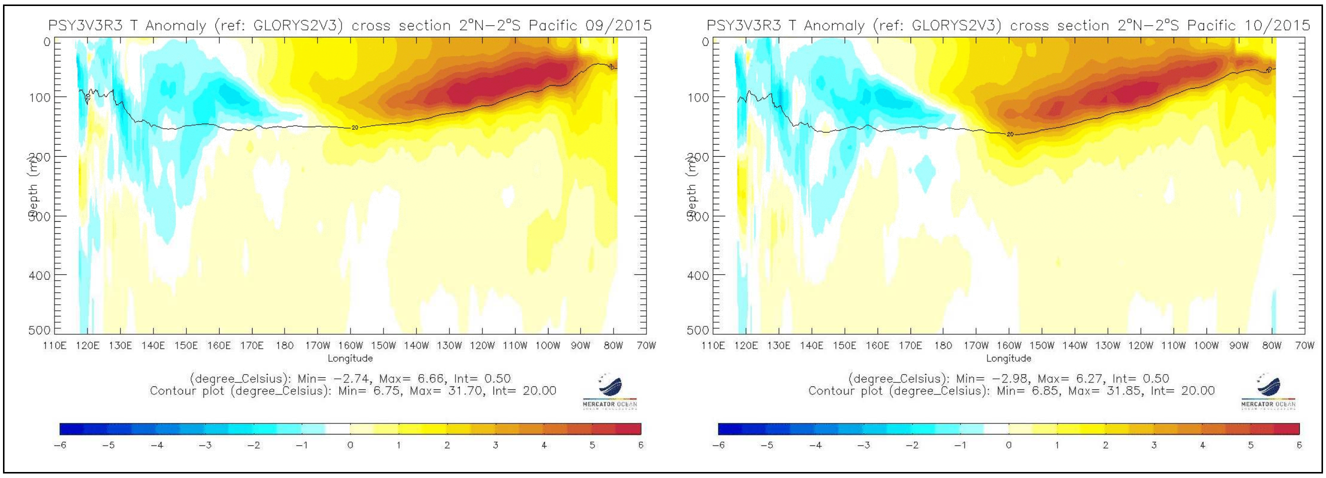

fig.I.1.4: Oceanic temperature anomaly in the first 500 meters in the Equatorial Pacific (previous and current month), http://bcg.mercator-ocean.fr

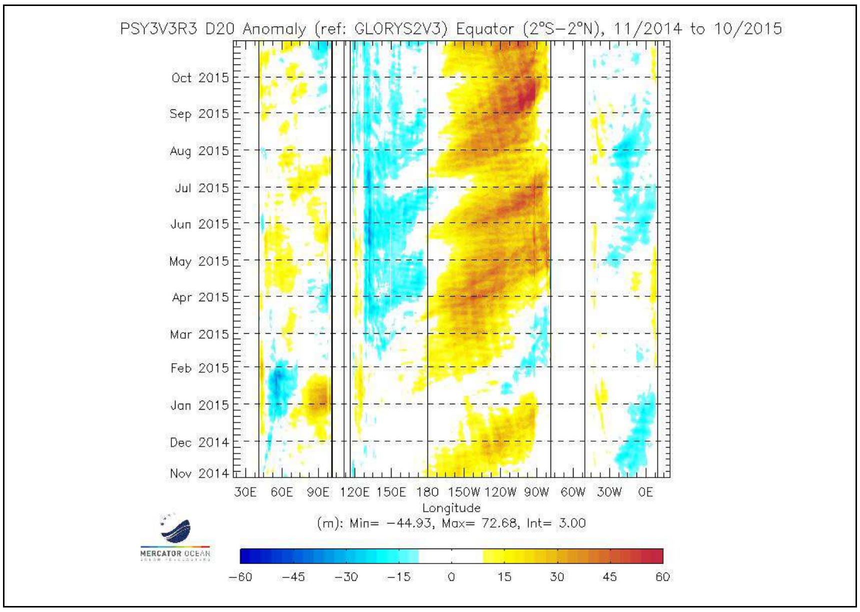

fig.I.1.5: Hovmüller diagram of Thermocline Depth Anomalies (m) (depth of the 20°C isotherm) along the equator for all oceanic basins over a 6 month period http://bcg.mercator-ocean.fr/

I.1.b Near Europe

Arctic Sea still warmer than normal, very high persistency.

Cold anomaly over the northern North Atlantic has shifted a little bit to the south. The North Sea has cooled less than normal from September to October, so anomalies are now about normal there. On the other hand, the cold anomaly has extended southwards to 30°N latitude.

There was also relatively little seasonal cooling of the Baltic Sea, anomalies are now well above normal, without any sea ice.

Eastern Mediterranean is still warmer than normal, whereas there was a relatively strong cooling over the northern parts of the western Mediterranean, which are now colder than normal.

Similarly relatively strong cooling over the Black Sea, but still mostly slightly above-normal anomalies.

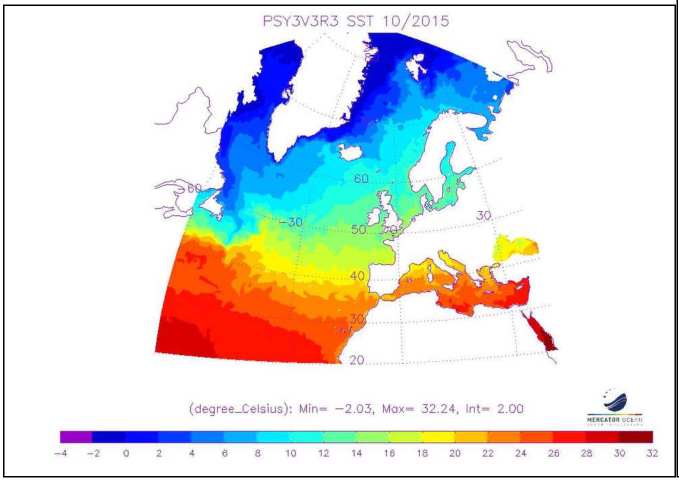

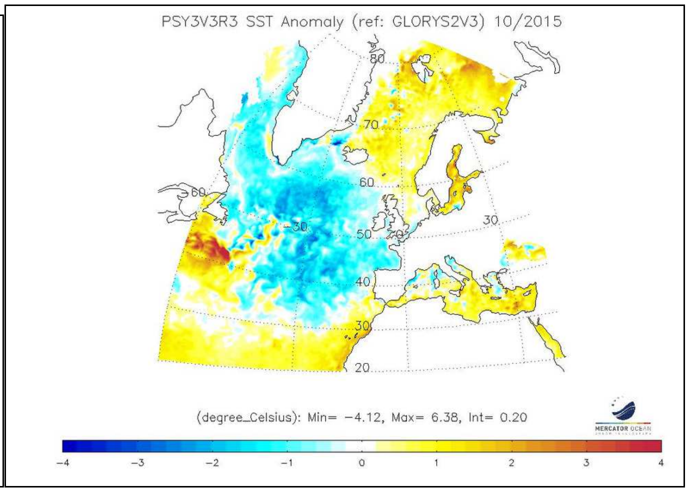

fig.I.1.6 : Mean sea surface temperature in the RA VI Region (Europe) and anomaly (reference Glorys 1992-2009). http://bcg.mercator-ocean.fr/

I.2.ATMOSPHÈRE

I.2.a General Circulation

Velocity Potential Anomaly field in the high troposphere (fig. 1.2.1 – insight into Hadley-Walker circulation anomalies) :

the anomaly pattern has remained very stable since September. MJO has little changed this pattern during the last week of October.

So still an intense dipole on the Pacific linked with ocean-atmosphere coupling related to El Nino. Large area of high upward motion anomaly on central and eastern Pacific, associated with positive SST anomalies. Conversely, large area of strong downward motion anomaly on the Southeast Asia, the Maritime Continent and Australia. Weaker downward motion anomaly area on the Caribbean and northern South America, and more diffuse upward motion anomaly on Africa.

Negative SOI index in October (-1.7), which abounds in the direction of ocean-atmosphere coupling (consistent with El Niño).

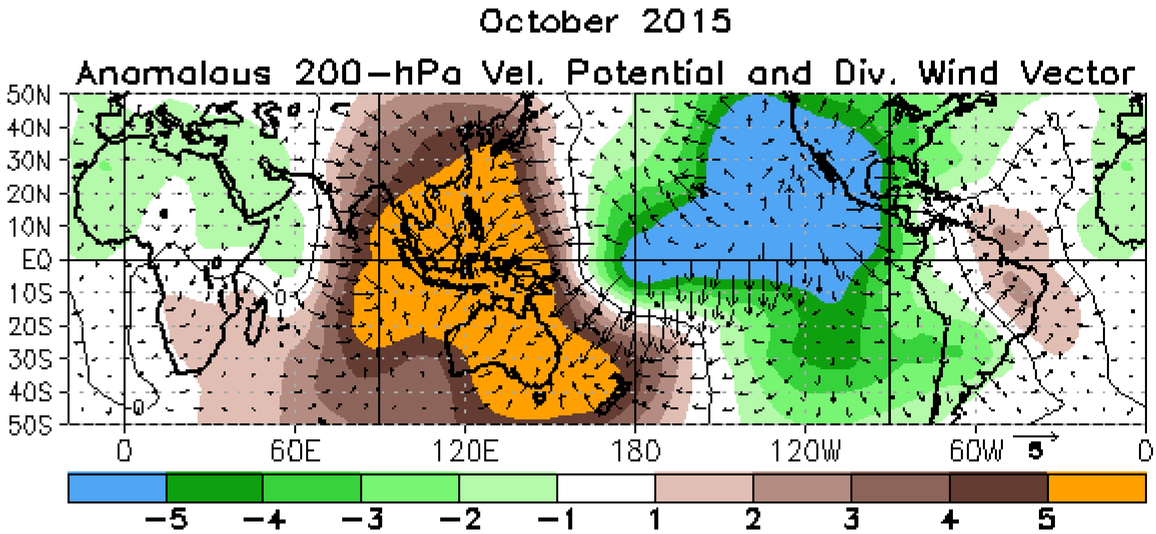

fig.I.2.1: Velocity Potential Anomalies at 200 hPa and associated divergent circulation anomaly. Green (brown) indicates a divergence-upward anomaly (convergence-downward anomaly).

http://www.cpc.ncep.noaa.gov/products/CDB/Tropics/figt24.shtml

MJO (fig. I.2.b):

MJO was active at the end of October, with limited impact on the velocity potential fields in the context of strong El Nino.

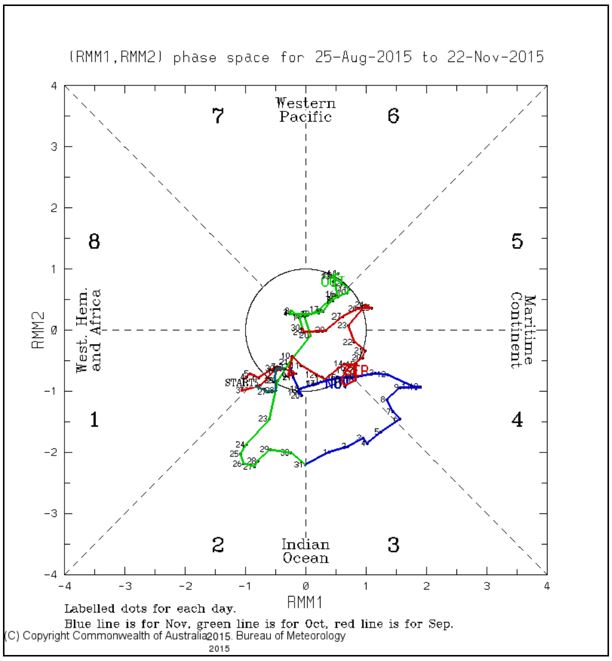

fig.I.2.b: indices MJO http://cawcr.gov.au/staff/mwheeler/maproom/RMM/phase.Last90days.gif

Stream Function anomalies in the high troposphere (fig. 1.2.2 – insight into teleconnection patterns tropically forced) :

Several similarities with September map.

Noticeable teleconnection in the Northern Pacific, corresponding to a typical response to El Nino (positive PNA pattern, PNA=2.1).

Over Indian Ocean, the cyclonic anomaly, North and South of the equator, could be reasonably linked to the large subsidence anomaly over the Maritime Continent.

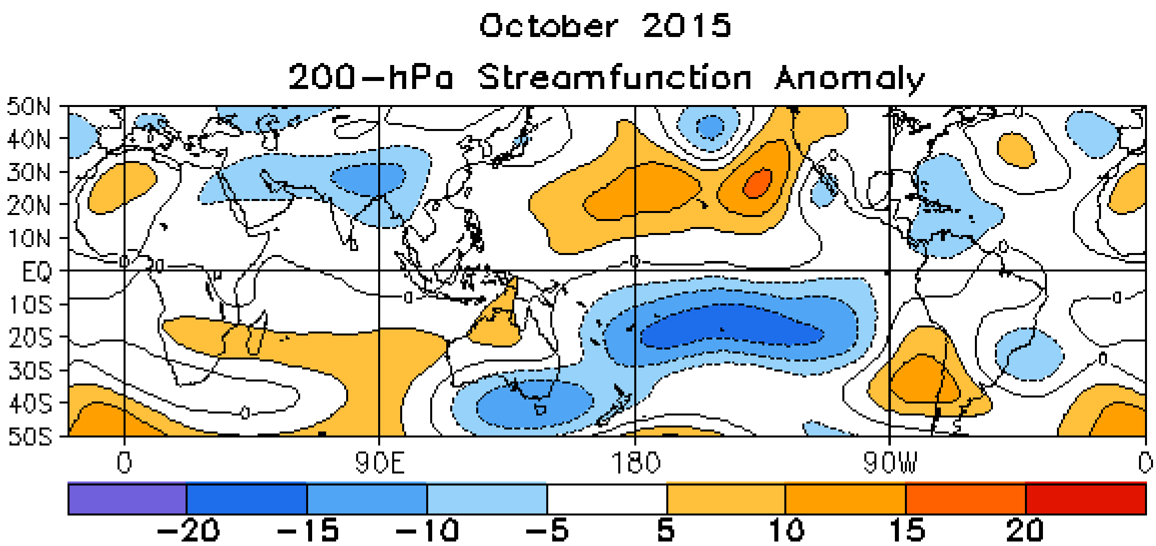

fig.I.2.2: Stream Function Anomalies at 200 hPa.

http://www.cpc.ncep.noaa.gov/products/CDB/Tropics/figt22.shtml

Geopotential height at 500 hPa (fig. 8 – insight into mid-latitude general circulation) :

PNA pattern very recognizable over Noth-America.

Over Northern Atlantic and Europe, blocking situation : vast negative anomaly SOuth-West of Greenland and Scandinavian blocking over Northern Europe. Nevertheless the dominant mode is NAO (value : +1), despite a non-zonal situation. The storm-track is moved Nothwestward.

Over the Mediterranean (Western part), significant negative anomaly.

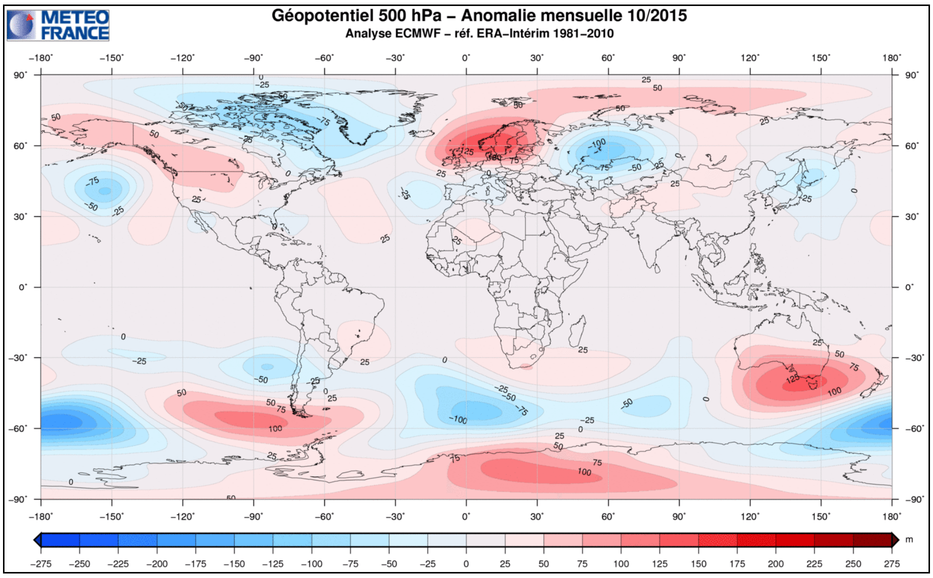

fig.I.2.3: Anomalies of Geopotential height at 500hPa (Meteo-France)

NAO	EA	WP	EP-NP	PNA	TNH	EATL/WRUS	SCAND	POLEUR	
-0.5	0.2	-1.4	-1.4	-0.8	-	-1.7	1.1	-0.1	September 15
1.0	0.2	-0.8	0.3	2.1	-	0.6	0.6	-0.5	October 15

Evolution of the main atmospheric indices for the Northern Hemisphere for the last 6 months :
http://www.cpc.ncep.noaa.gov/products/CDB/Extratropics/table3.shtml

Sea level pressure and circulation types over Europe

Zonal air flow over the North Atlantic with slightly higher-than-normal Icelandic Low. Since October, NAO has switched to a positive phase (index 1.0). Blocking High over Europe, much extended to the north, therefore highest anomalies over Scandinavia, explained by a still positive SCAND pattern (+0.6), but this has weakened compared to September 2015. Nevertheless, days with blocking situation dominated throughout the months. Another contribution comes from EATL/WRUS pattern (equally high with also +0.6) with a negative anomaly over Russia and a positive anomaly over the North Sea.

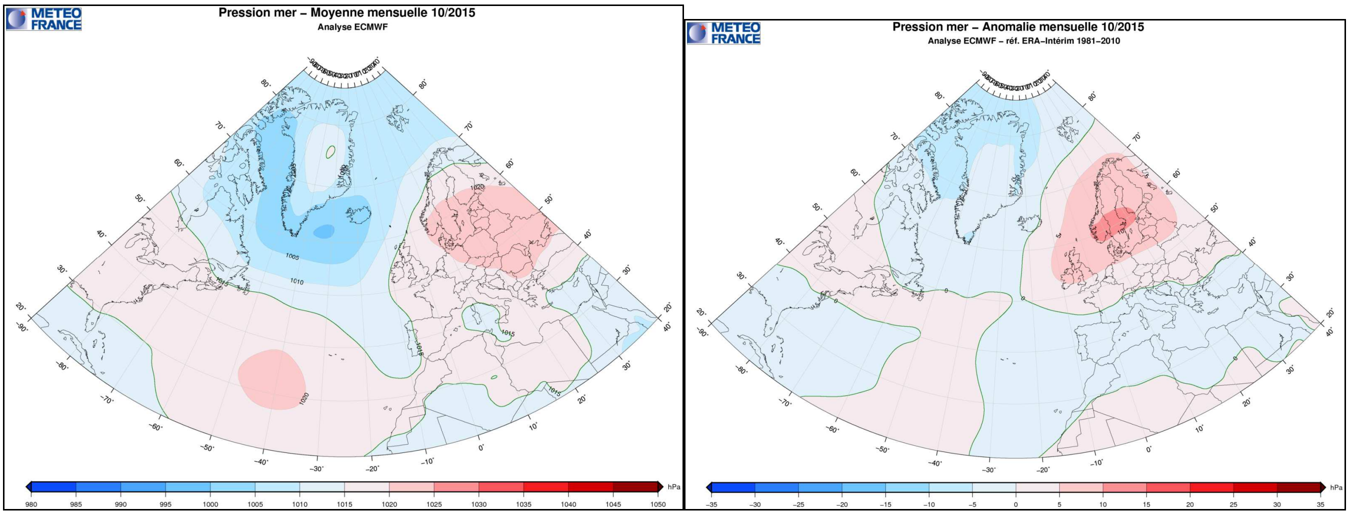

fig.I.2.4: Mean sea level pressure in the RA VI Region (Europe) (top) and 1981-2010 anomalies (bottom).

Circulation indices: NAO and AO

NAO started around zero at the beginning of the month, but a significant positive phase developed particularly in the second half of October and continued also in November. This points to some general tendency to more zonality over the North Atlantic during autumn season. AO had a negative peak in the first half of October, but oscillated around zero in the second half. This means some above-normal air mass exchange between polar and middle latitudes in the first half of the month, but only temporarily.

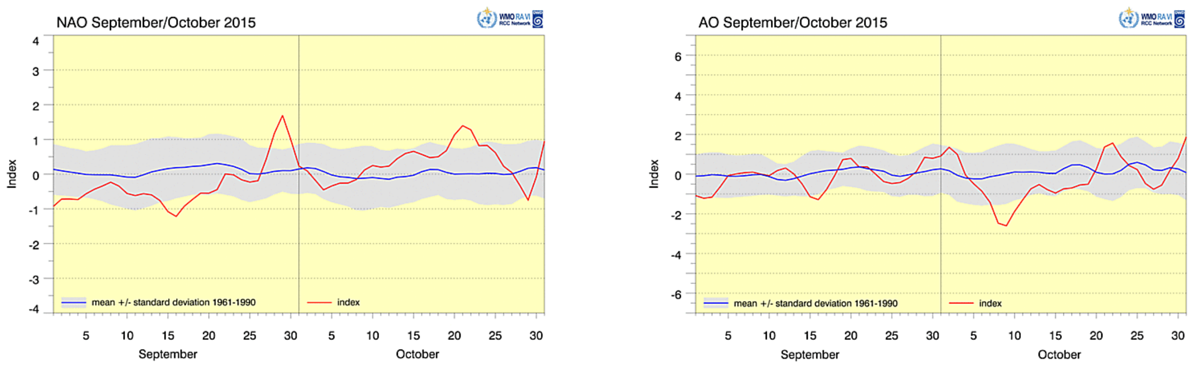

fig.I.2.5: North Atlantic Oscillation (NAO, left) and Arctic Oscillation (AO, right) indices with 1961-1990 mean standard deviation (shading). http://www.dwd.de/rcc-cm , data from NOAA CPC: http://www.cpc.ncep.noaa.gov/products/precip/CWlink/daily_ao_index/teleconnections.shtml

I.2.b Precipitation

The strongest anomalies are those conventionally expected in the Niño current phase, with a surplus of precipitation over the central and eastern equatorial Pacific and marked deficit on the Maritime Continent, and Central America, the Caribbean, northern South America.

The end of the African monsoon was rather surplus in its western part.

Over Europe, South-North gradient clearly linked to the geopotentiel pattern (Scandinavian blocking).

.

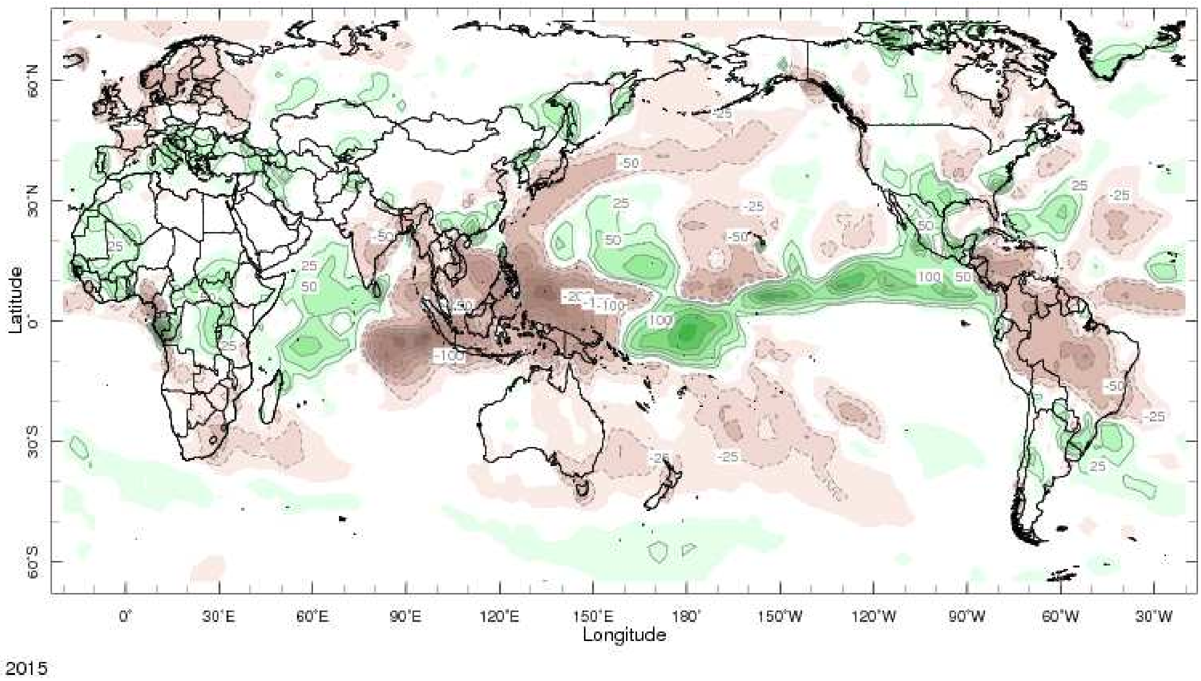

fig.I.2.4: Rainfall Anomalies (mm) (departure to the 1979-2000 normal) – Green corresponds to above normal rainfall while brown indicates below normal rainfall.

http://iridl.ldeo.columbia.edu/maproom/.Global/.Precipitation/Anomaly.html

Precipitation anomalies in Europe:

Most of western and northern Europe very dry, especially a region from southern Norway to the Baltic countries and further to eastern Ukraine with partly extreme drought conditions, much in line with highest geopotential and SLP anomalies of Scandinavian High. In contrast, some areas with particularly high vertical upward motion and heavy precipitation in southern Europe / Mediterranean, namely over Portugal, Italy/Balkans and eastern Turkey / South Caucasus.

This dipole was mainly caused by SCAND pattern, but modified by local systems of high intensity in the south.

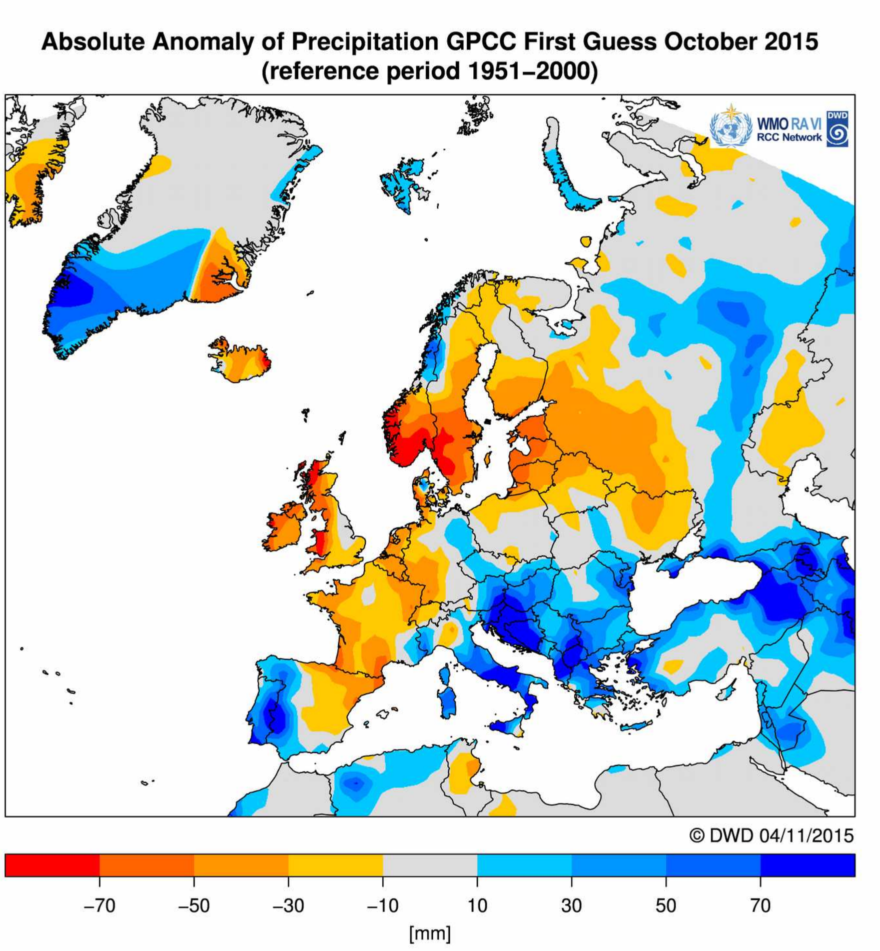

fig.I.2.5: Left: Absolute anomaly (1951-2000 reference) of precipitation in the RA VI Region (Europe), data from GPCC (Global Precipitation Climatology Centre), http://www.dwd.de/rcc-cm. Right: Percentiles of precipitation, 1981-2010 reference. Data from NOAA Climate Prediction Center, http://iridl.ldeo.columbia.edu/maproom/Global/Precipitation/Percentiles.html

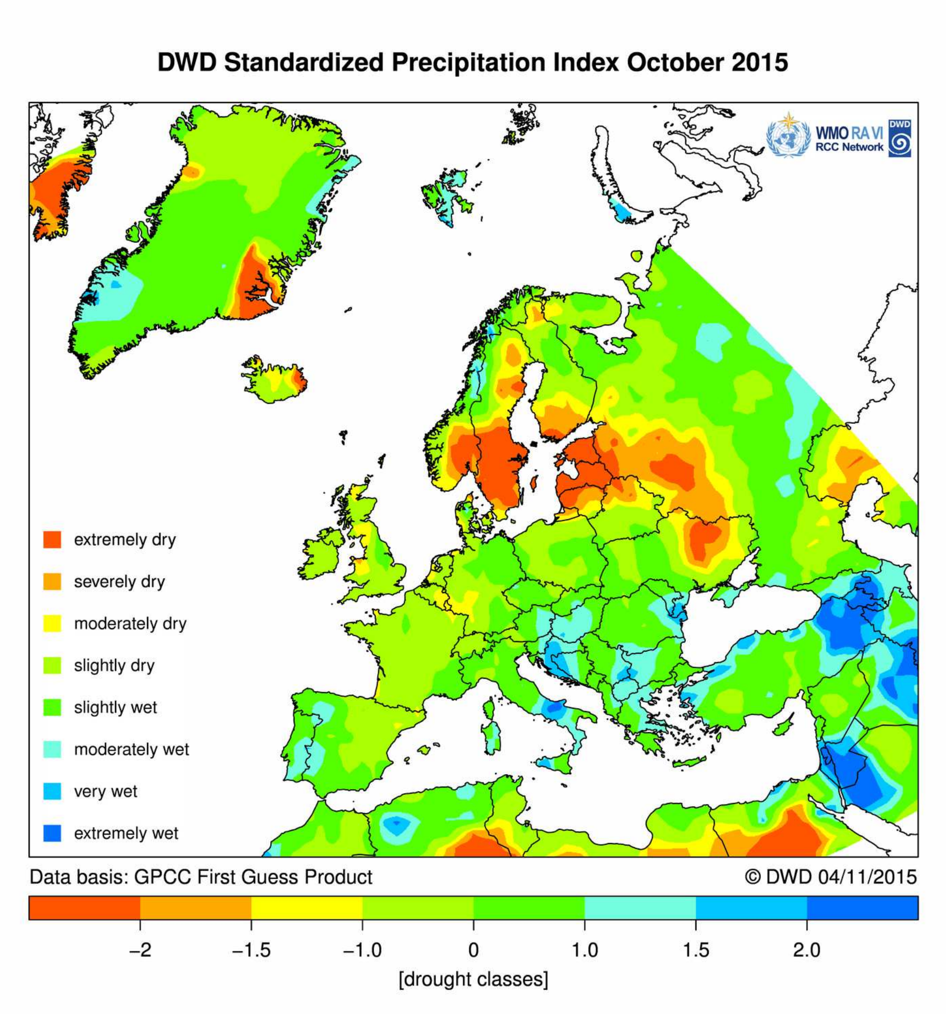

fig. I.2.5a: Standardized Precipitation Index with DWD modification (DWD-SPI), http://www.dwd.de/rcc-cm .

Monthly mean precipitation anomalies in European subregions. Subregions refer to ECMWF land boxes defined in Annex III.3. Anomalies are based on gridded data from GPCC First Guess Product, ftp://ftp-anon.dwd.de/pub/data/gpcc/PDF/GPCC_intro_products_2008.pdf, 1951-2000 reference.

Subregion	Absolute anomaly	SPI DWD Drought Index
Northern Europe	- 37 mm	-0.98
Southern Europe	+18 mm	+ 0.42

I.2.c Temperature

Consistant with geopotential, warm anomaly on Northern Europe (British islands to Scandinavia), cold anomaly elsewhere. And warm anomaly over the Mediterranean basin.

Warm anomaly in the northern two-thirds of South America. Combined effect of PDO and PNA pattern : warm anomaly over a large part of the United States and western Canada, cold anomaly on eastern Canada.

.

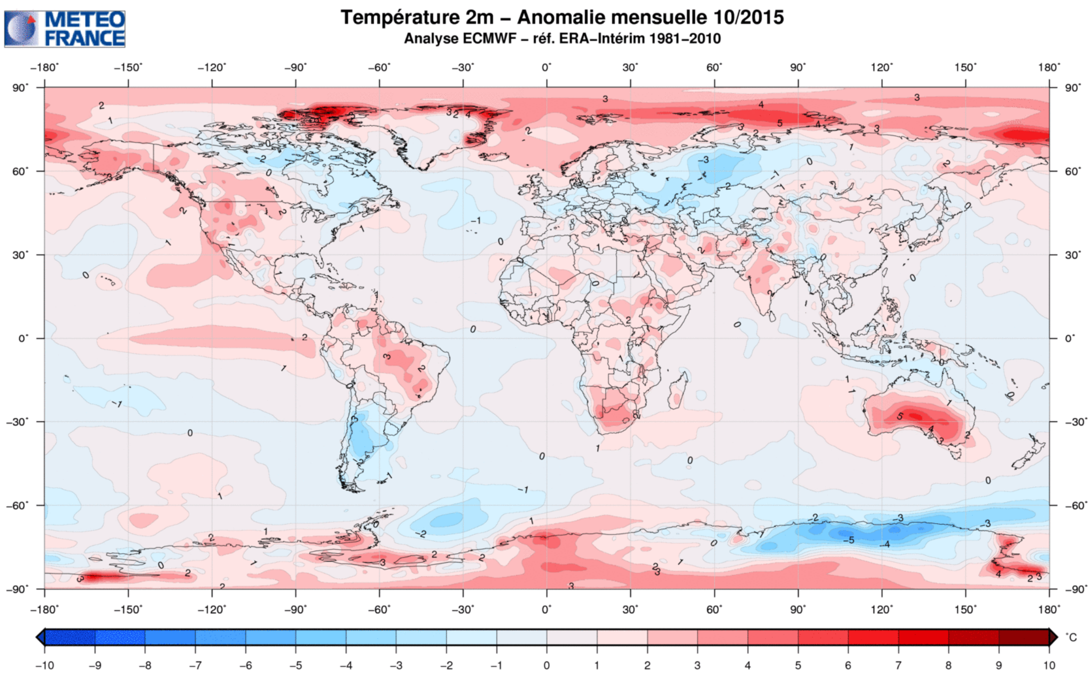

fig.I.2.8: Temperature Anomalies (°C) (Meteo-France)

<u>Temperature anomalies in Europe:</u>

Arctic and northern Europe mild, colder than normal in central latitudes, warmer than normal in the south. Polar air moved to Eastern Europe east of the Scandinavian High, and then to central and western Europe in an easterly flow south of this High, particularly around the middle of October. In contrast, the zonal airflow component over the North Atlantic was redirected to the north due to the Scandinavian blocking, leading mild air to the Arctic region. Southern Europe /Mediterranean mainly influenced by subtropical air masses, in spite of some local cooling due to some intense cyclones.

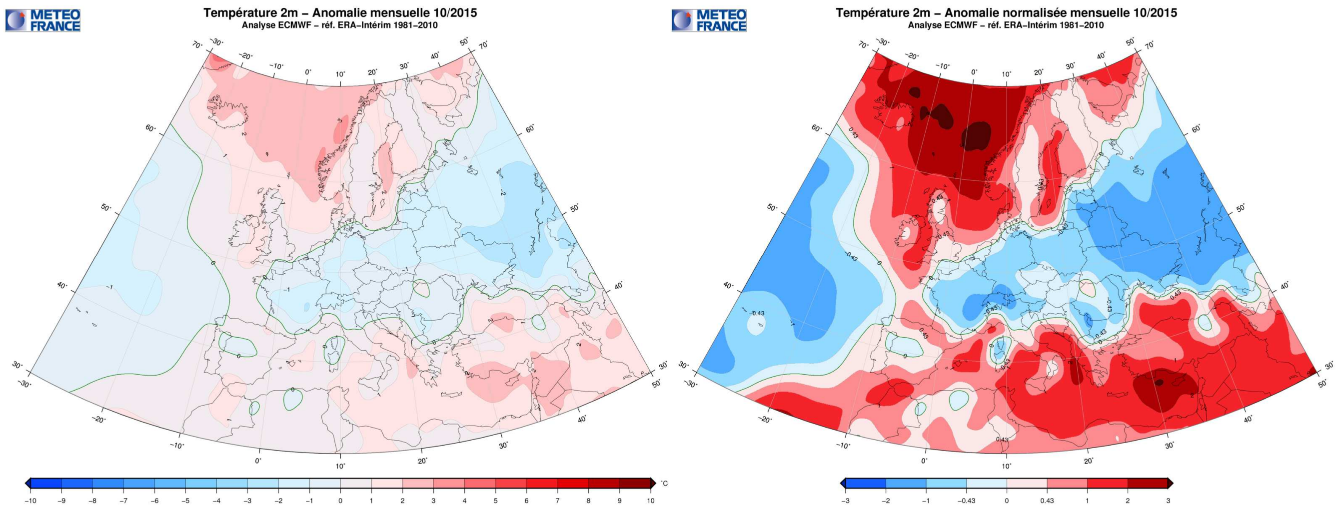

fig.I.2.9: Left graph: Absolute anomaly of temperature in the RA VI Region (Europe). Right graph: Standardized temperature anomalies

Monthly mean temperature anomalies in European subregions: Subregions refer to ECMWF land boxes defined in Annex III.3. Anomalies are based on gridded CLIMAT data from DWD, http://www.dwd.de/rcc-cm, 1961-1990 reference.

Subregion	Anomaly
Northern Europe	+0.4°C
Southern Europe	+0.5°C

I.2.d Sea ice

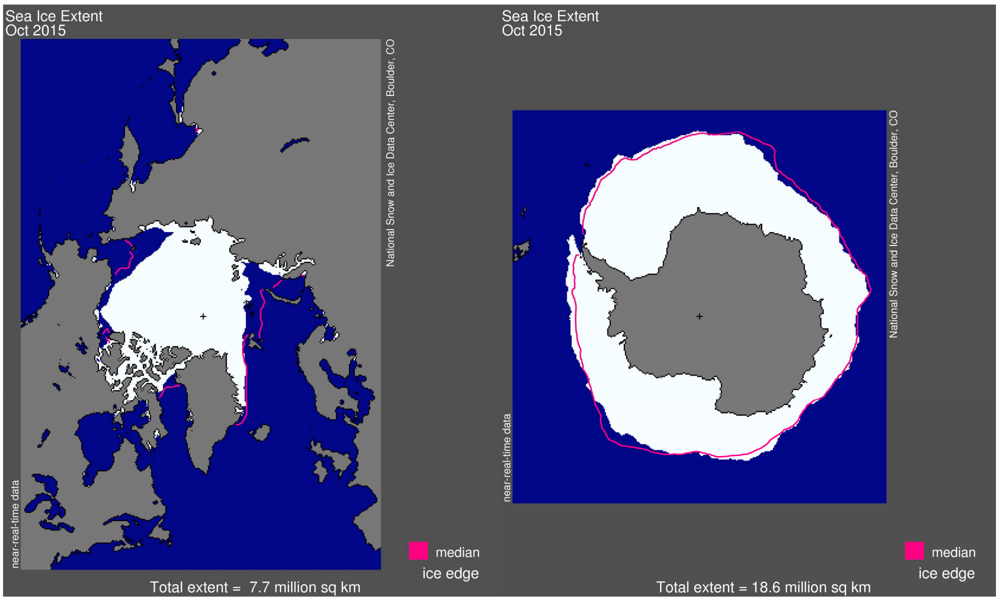

fig.I.2.15: Sea-Ice extension in Arctic (left), and in Antarctic (right). The pink line indicates the averaged extension (for the 1979-2000 period). http://nsidc.org/data/seaice_index/

In Arctic (fig. 1.2.15 and 1.2.16 - left): persistent significant deficit (~ -2 std). Northeast and Northwest passages closed.

In Antarctic (fig. 1.2.15 and 1.2.16 - right): near normal values.

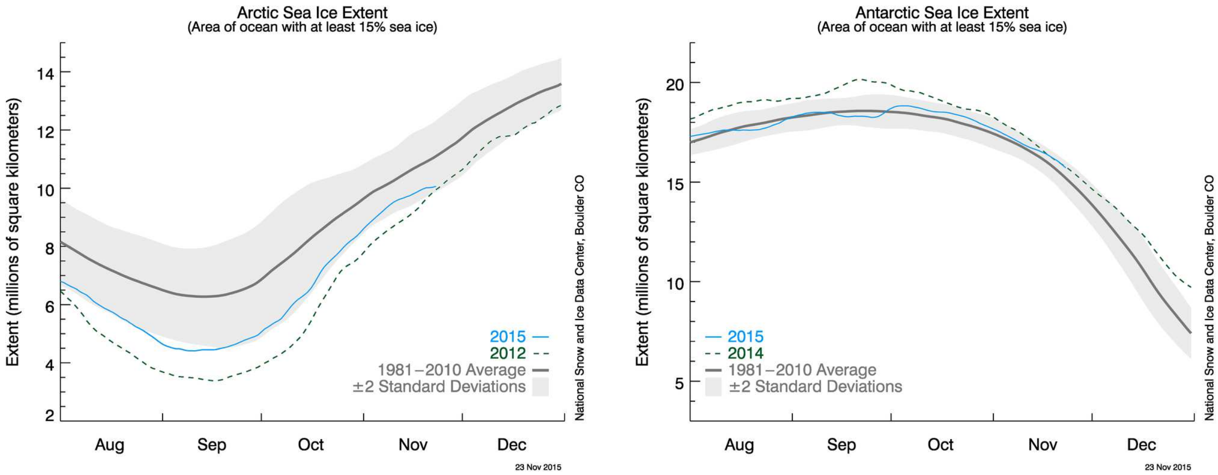

fig. I.2.16 : Sea-Ice extension evolution from NSIDC.

http://nsidc.org/data/seaice_index/images/daily_images/N_stddev_timeseries.png

II. SEASONAL FORECAST FROM DYNAMICAL MODELS

II.1. OCEANIC FORECASTS

The global climate system is strongly influenced by the current El Nino event. In that condition, the predictability is significantly strengthened in the tropical area, but seems also much better than usual in some regions mid-latitudes. All seasonal forecast models are very close in the tropics, particularly EUROSIP models. The anomaly patterns are very consistent both for the ocean and for the atmosphere in the tropical areas.

II.1.a Sea surface temperature (SST)

Pacific Ocean: remaining of the warm anomaly in central and eastern Equatorial Waveguide, this is the maximum of the event. The large area of warm anomaly will also persist along the western coast of North America to the Bering Strait, due to the positive PDO phase.

Persistence of the cold anomaly in the Southern Hemisphere, from the Solomon Islands to New Zealand south on one hand, and with an extension towards the east until about 90W on the other hand. Interestingly, all models forecast a significant warming around the maritime continent.

Indian Ocean: Remaining of the generalized warm anomaly, particularly strong in the south of the Tropic of Capricorn. Many models forecast an evolution toward a neutral or negative DMI (currently positive), this is quite unusual during strong El Nino events.

Atlantic Ocean: As in previous months, the tropical Atlantic is the only area where models diverge significantly with a very clear difference between ECMWF and ARP on one hand (warm anomalies), and NCEP on the other hand (significant cold anomaly) . The EUROSIP average is rather negative but unreliable in this area. The models agree on the persistence of the strong cold anomaly on the North Atlantic and of warm anomaly from Caribbean and American coasts to Africa.

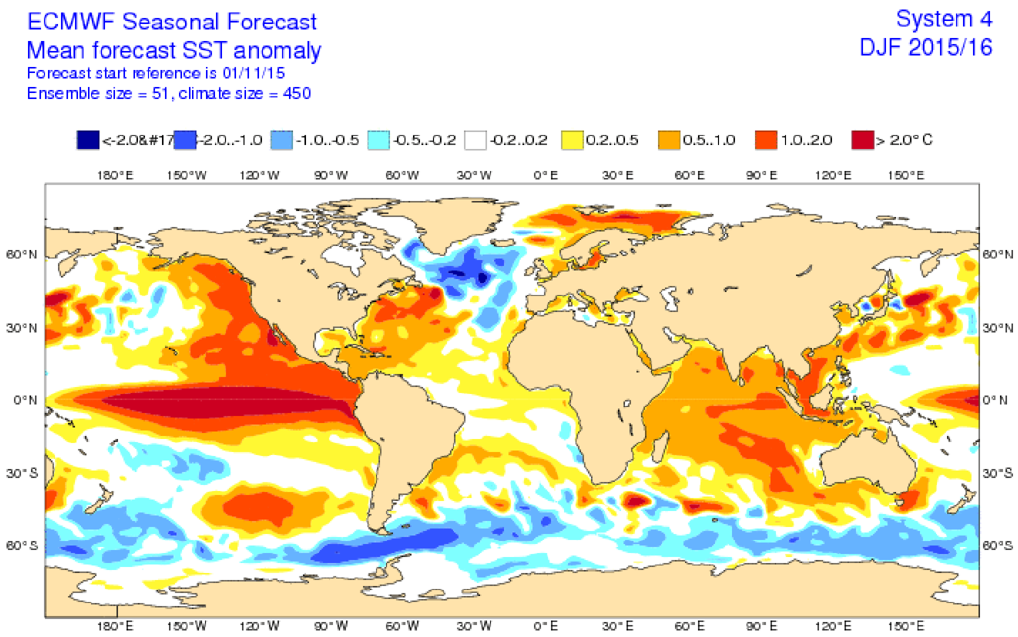

fig.II.1.1: SST anomaly forecast from ECMWF

http://www.ecmwf.int/products/forecasts/d/charts/seasonal/forecast/seasonal_range_forecast/group/

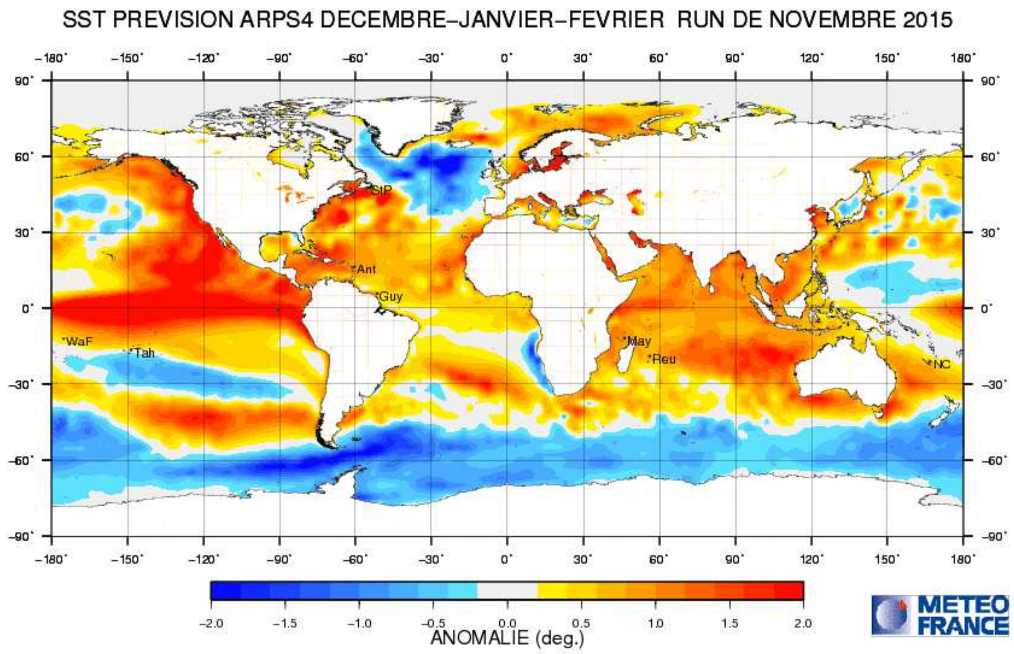

fig.II.1.2: SST Anomaly forecast from Meteo-France (recalibrated with respect of observation).

http://elaboration.seasonal.meteo.fr

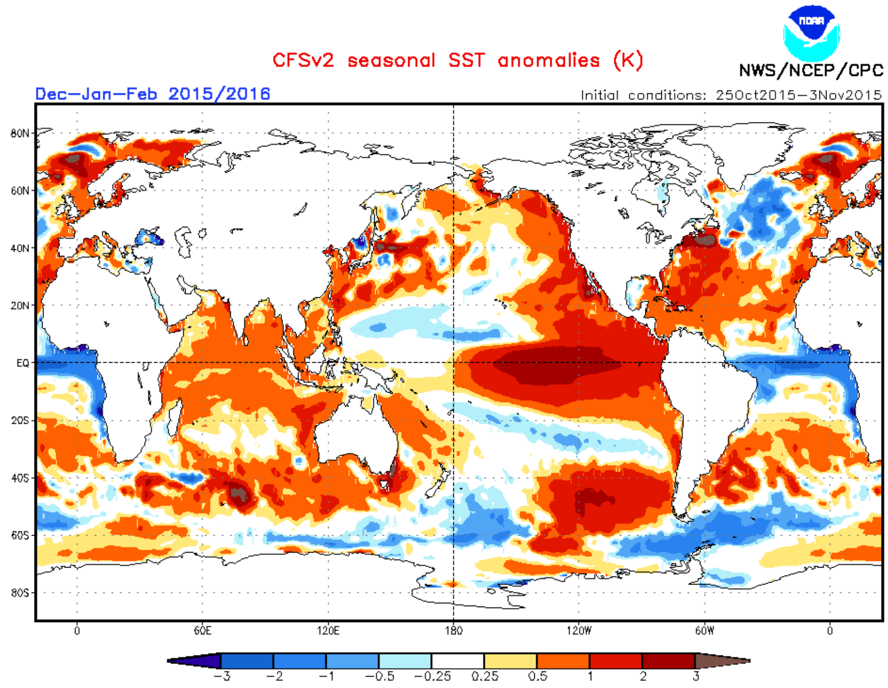

fig.II.1.3: SST anomaly forecast from NCEP.

http://www.cpc.ncep.noaa.gov/products/people/wwang/cfsv2fcst/imagesInd1/glbSSTSeaInd1.gif

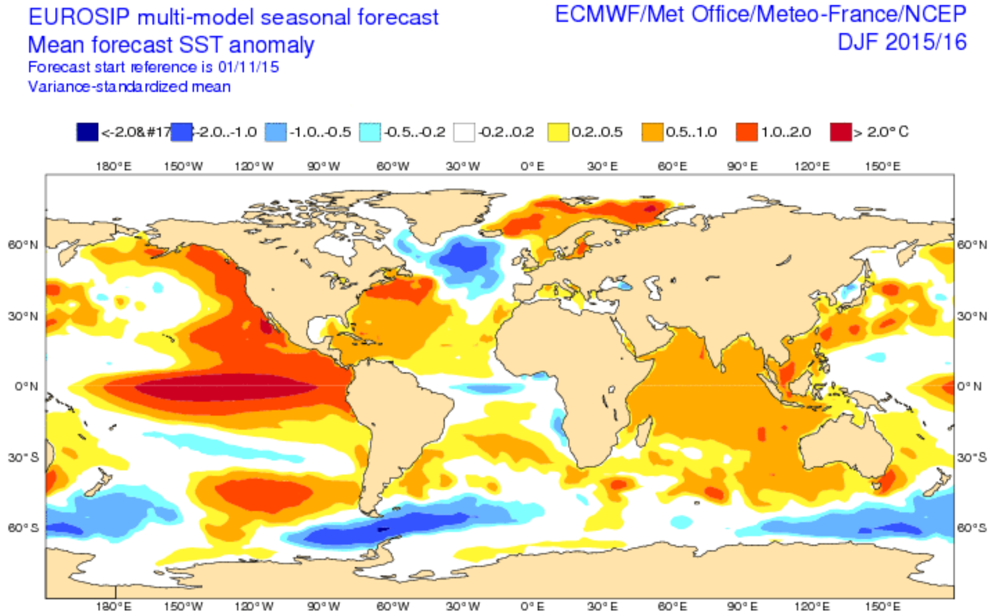

fig.II.1.4: SST Forecasted anomaly from Euro-SIP

II.1.b ENSO forecast

Forecast Phase: very strong El Niño event

Very good consistency between models in the strength of El Nino. The SST anomaly in Niño3.4 box should follow a classic path and reach its maximum in November-December, and start decreasing in January. The average maximum value on a quarter (according to the ONI) should be similar to the event record for 1997/1998. http://www.cpc.noaa.gov/products/analysis_monitoring/ensostuff/ensoyears.shtml .

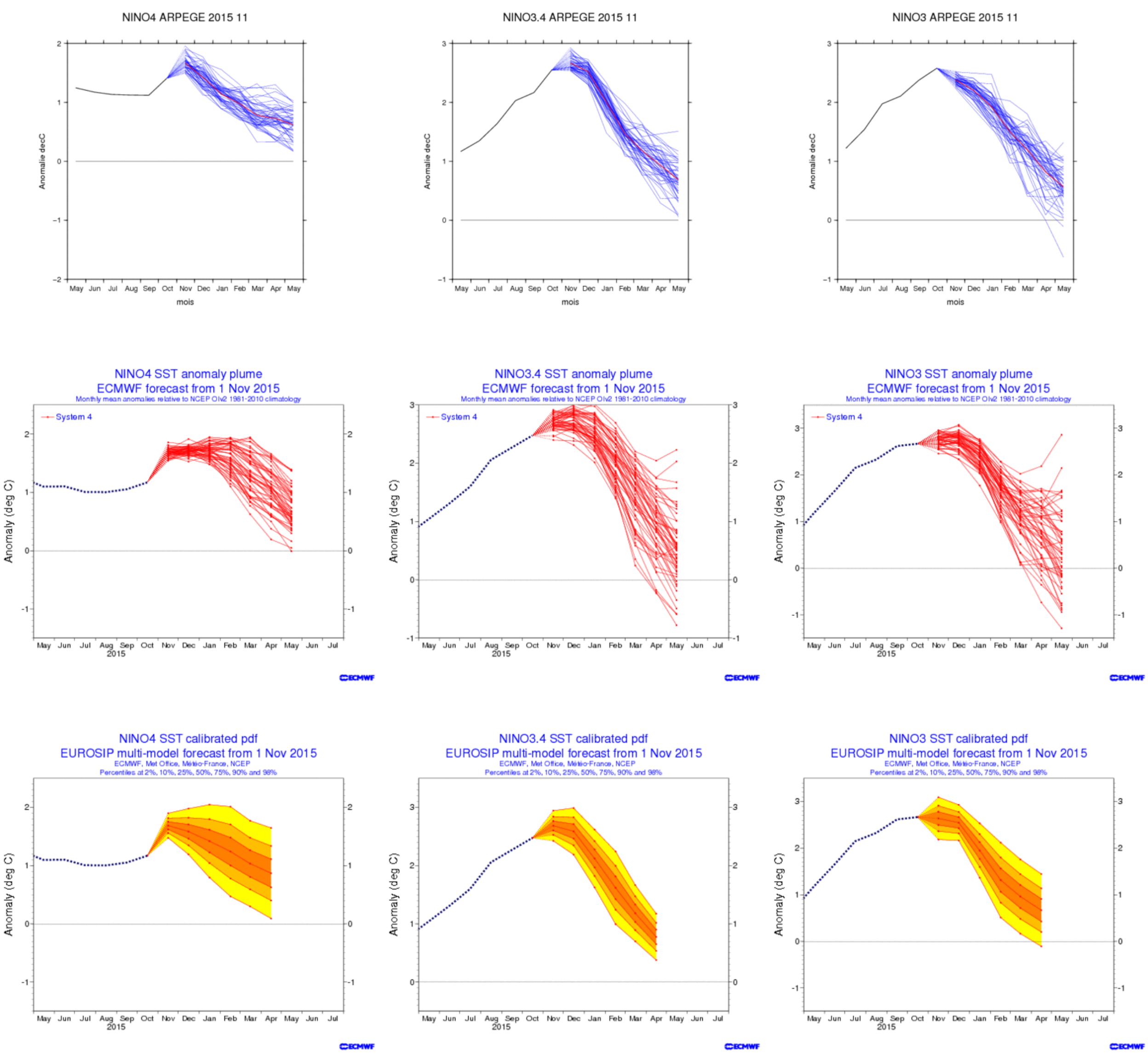

fig.II.1.5: SST anomaly forecasts in the Niño boxes from Météo-France (top) and ECMWF (middle) - monthly mean for individual members - and EuroSIP (bottom) – recalibrated distributions - (http://elaboration.seasonal.meteo.fr , http://www.ecmwf.int/)

II.1.c Atlantic ocean forecasts

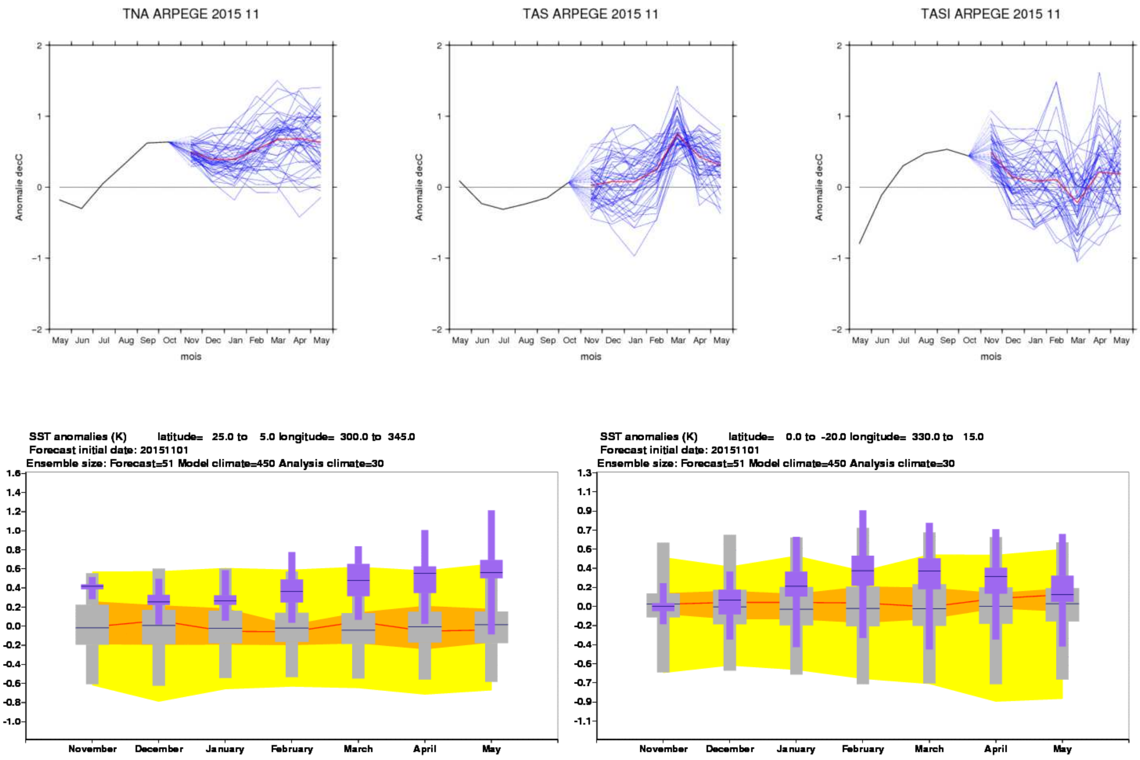

fig.II.1.6: SSTs anomaly forecasts in the Atlantic Ocean boxes from Météo-France and ECMWF, plumes / climagrams correspond to ensemble members and monthly means.

II.1.d Indian ocean forecasts

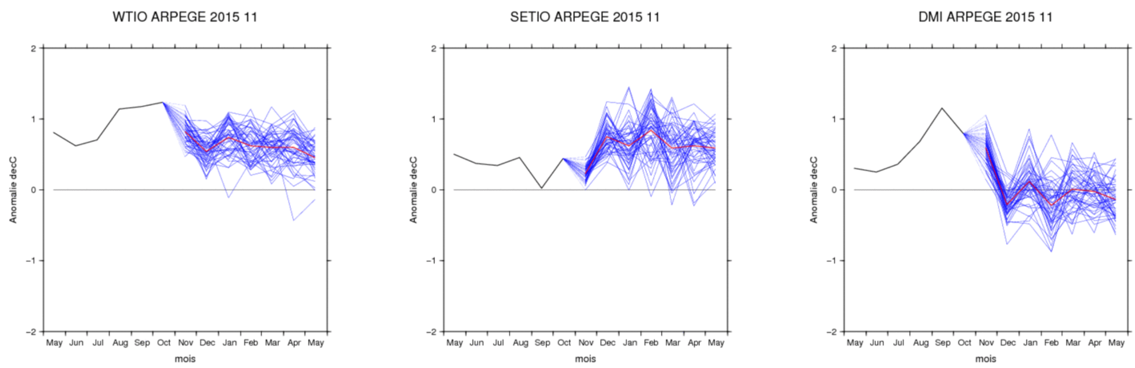

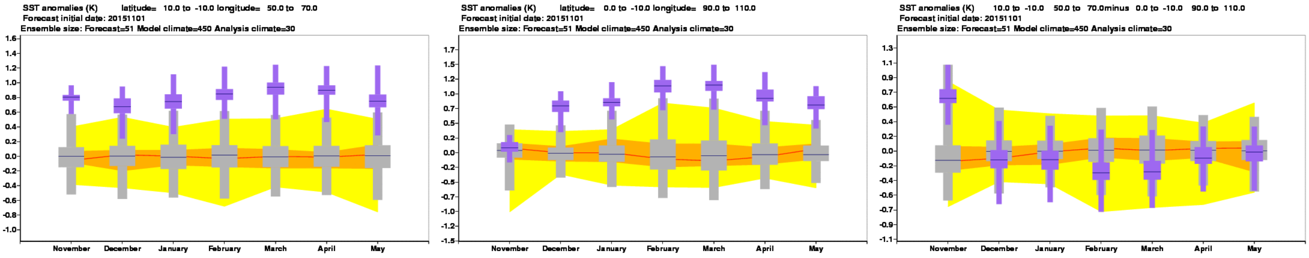

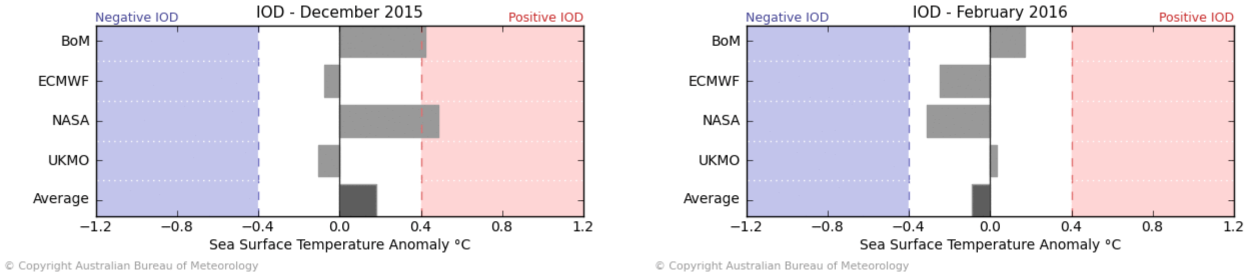

fig.II.1.7: SSTs anomaly forecasts in the Indian Ocean boxes from Météo-France and ECMWF, plumes / climagrams correspond to ensemble members and monthly means.

II.2. GENERAL CIRCULATION FORECAST

II.2.a Global forecast

Velocity potential anomaly field (cf. fig. II.2.1 – insight into Hadley-Walker circulation anomalies): Strong and consistent signal, with a major dipole linked to El Nino, with a very strong downward anomaly area on Maritime Continent and a vaste upward motion area on central and eastern Pacific Ocean. Note that this upward motion anomaly is divided in 2 maxima, the 1st one centered around 150°W and the second one in the Northern hemisphere, extending from Pacific to Central America : this is typical what the pattern exhibits by composite of El Nino events in DJF.

The other anomalies are very similar in MF, ECMWF and JMA : + over Brazil, - south of India, +/- dipole over Africa.

Stream Function anomaly field (cf. fig. II.2.1 – insight into teleconnection patterns tropically forced):

The models are close in the intertropical belt, this strong anomalies in tropical regions. We see again a quadripole in the tropical Pacific Ocean and Eastern Indian Ocean, clearly linked to major velocity potentail anomalies over the Maritime Continent and the central Pacific Ocean. The 3 models are forecasting a clear teleconnection from Pacific to Canada (PNA pattern). Over Atlantic Ocean, models are consistent in the tropics, they show some differences in intensity in higher latitudes, especially close to Europe).

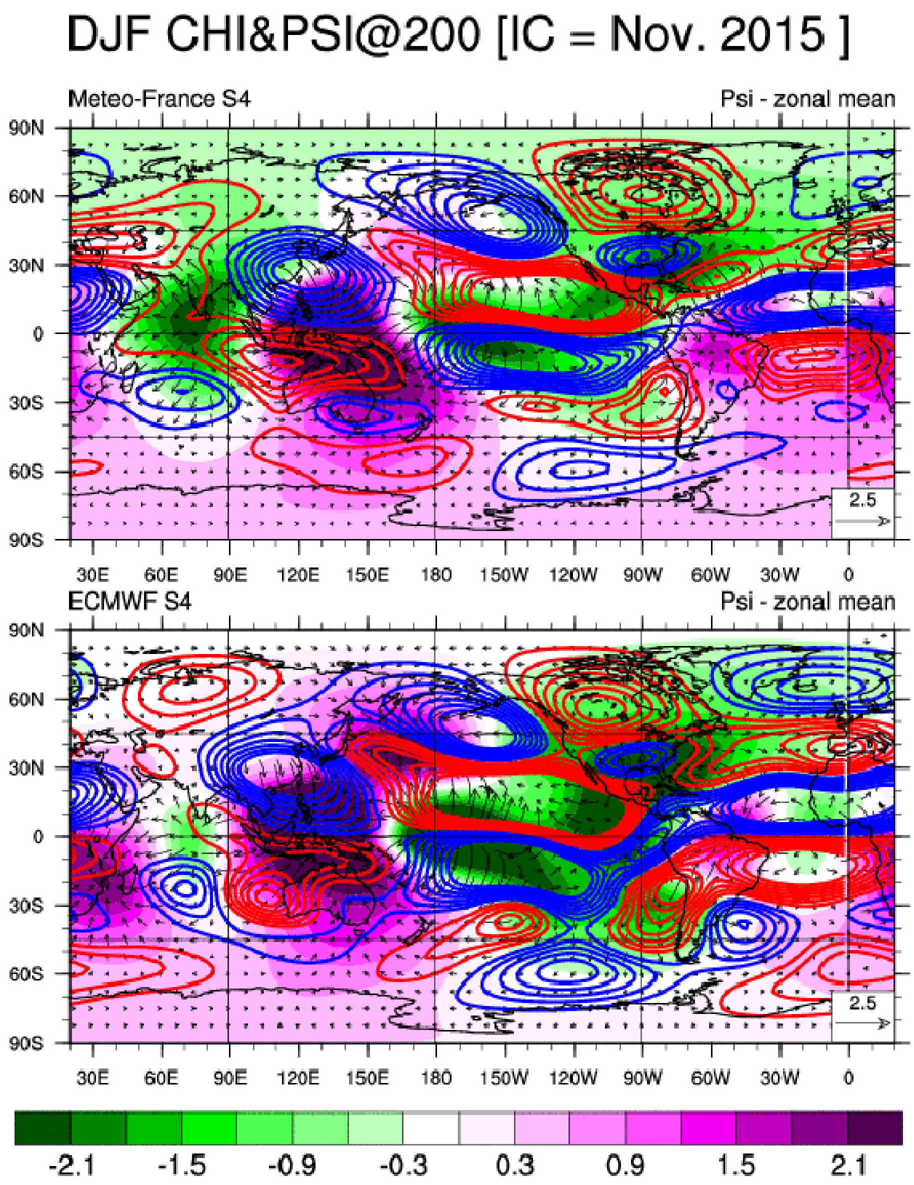

fig.II.2.1: Velocity Potential anomaly field χ (shaded area – green negative anomaly and pink positive anomaly), associated Divergent Circulation anomaly (arrows) and Stream Function anomaly ψ (isolines – red positive and blue negative) at 200 hPa by Météo-France (top) and ECMWF (bottom).

II.2.b North hemisphere forecast and Europe

Geopotential height anomalies (fig. II.2.2 – insight into mid-latitude general circulation anomalies): Very strong anomalies in MF and ECMWF, consequence of lower dispersion than usual between members of each model. And we can find most geopotential anomaly kernels on both models. The differences in intensity are quite important close to Europe, especially the negative anomaly close to the British Isles. As a consequence, anomalous regime occurrences are opposite between MF and ECMWF concerning NAO+ and NAO- regimes. However, one can note that in both models, blocking regimes are less frequent than usual.

Looking at other GPC forecasts, we can't find a more probable mode in Northern Atlantic. The dominant idea is a circulation stronger than usual, corresponding to a positive NAO (as ECMWF or UKMO) or a more South-Western anomaly circulation (like MF or BOM).

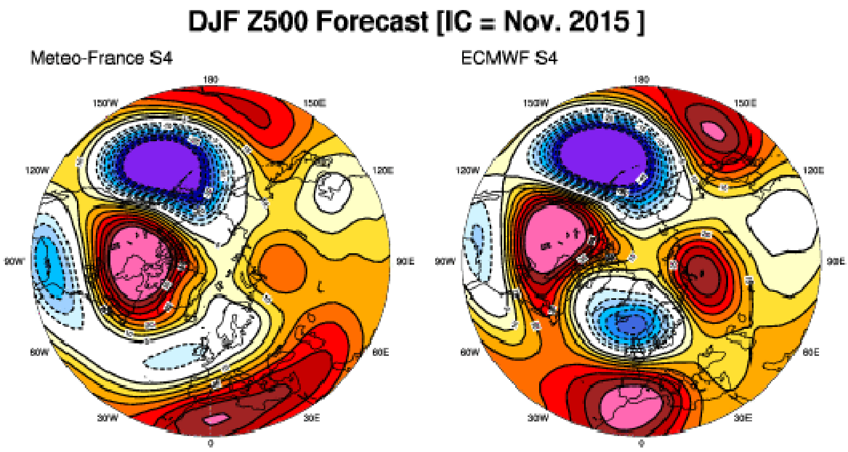

fig.II.2.2: Anomalies of Geopotential Height at 500 hPa from Météo-France (left) and ECMWF (right).

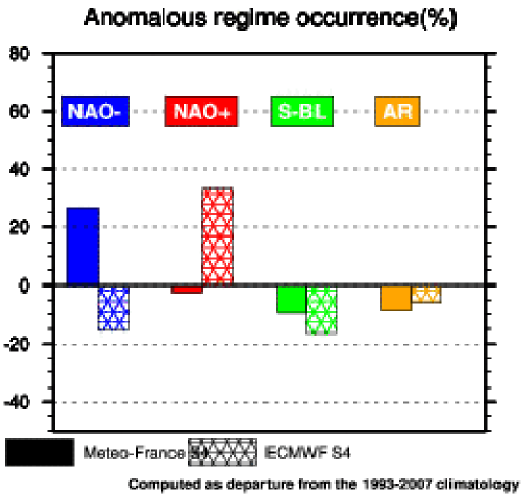

fig.II.2.3: North Atlantic Regime occurrence anomalies from Météo-France and ECMWF : vertical bars represent the excitation frequency anomaly (in %) for each of the 4 regimes.

II.3. IMPACT: TEMPERATURE FORECASTS

Besides global warming, the ENSO+ and PDO+ context and Indian Ocean SST anomalies are favorable to enhanced probability of global warm anomaly. The few exceptions are on sea areas where surface temperatures are provided below normal, and on land : Greenland, Mexico and the southern United States, Argentina.

On Europe, a "warmer than normal" signal is most likely, except the British Isles. This is consistent with general circulation.

II.3.a ECMWF

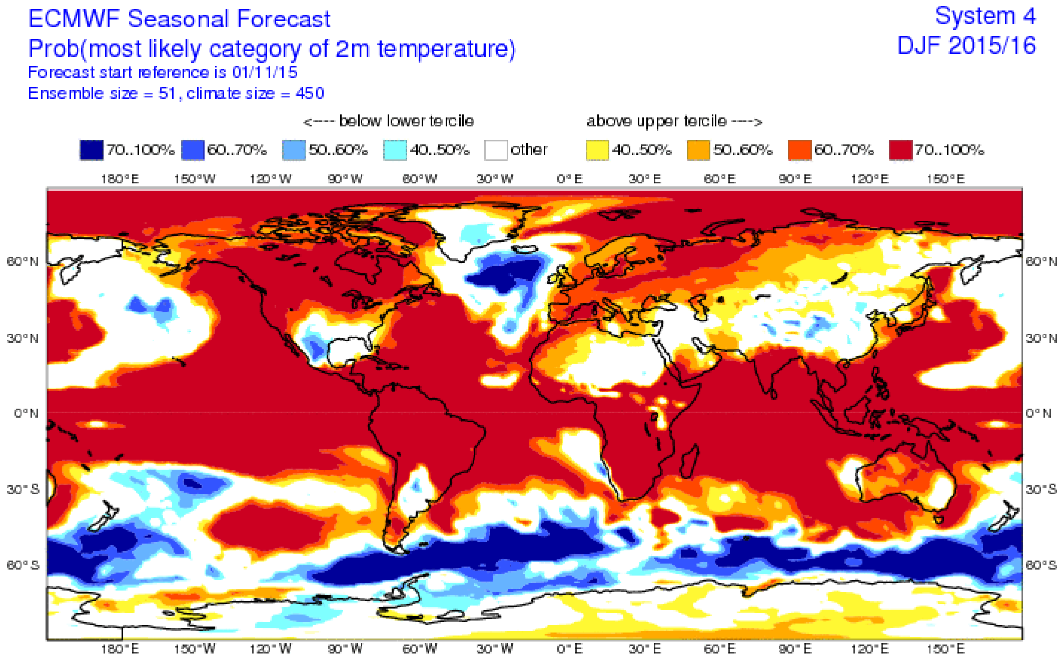

fig.II.3.1: Most likely category probability of T2m from ECMWF. Categories are Above Normal, Below Normal and « other » category (Normal and No Signal). http://www.ecmwf.int/products/forecasts/d/charts/seasonal/forecast/

II.3.b Météo-France

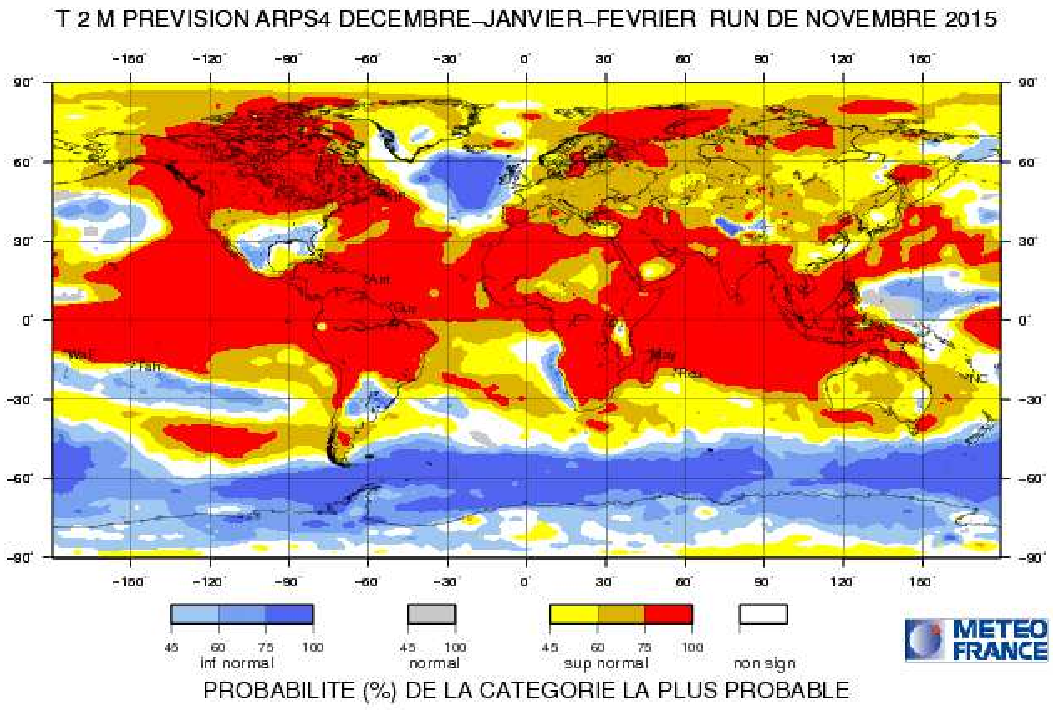

fig.II.3.2: Most likely category of T2m. Categories are Above, Below and Close to Normal. White zones correspond to No Signal. http://elaboration.seasonal.meteo.fr/

II.3.c Japan Meteorological Agency (JMA)

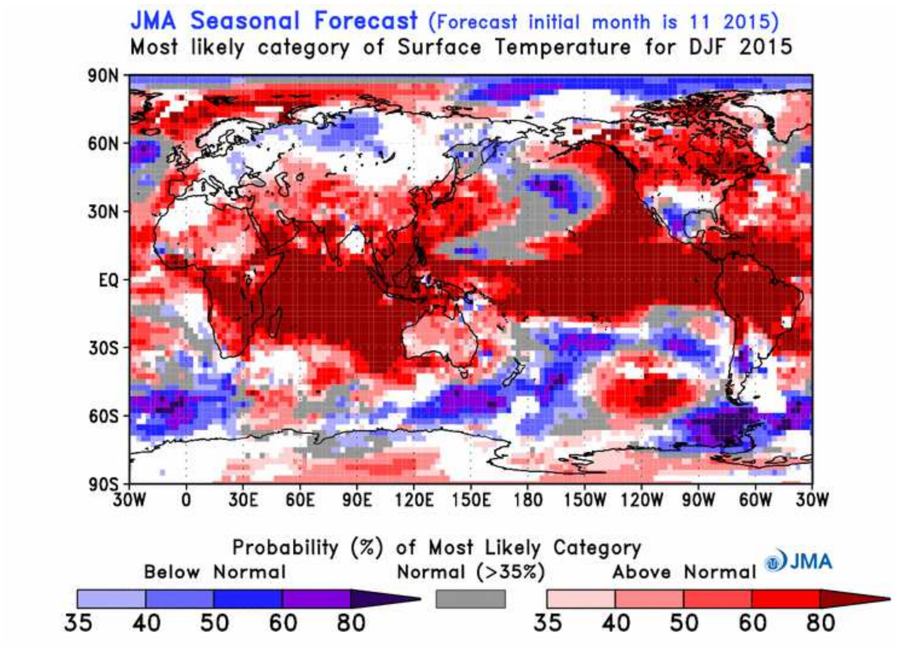

fig.II.3.3: Most likely category of T2m. Categories are Above, Below and Close to Normal. White zones correspond to No Signal. http://ds.data.jma.go.jp/tcc/tcc/products/model/probfcst/4mE/fcst/fcst_gl.php

II.3.d EUROSIP

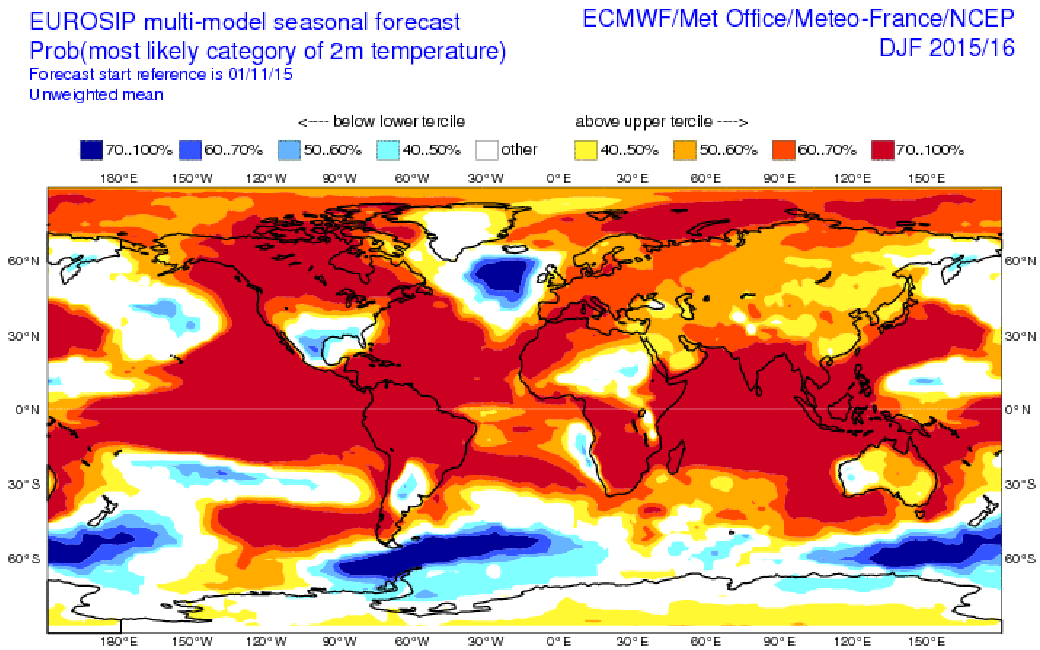

fig.II.3.4: Multi-Model Probabilistic forecasts for T2m from EUROSIP (2 Categories, Below and Above normal – White zones correspond to No signal and Normal).
http://www.ecmwf.int/products/forecasts/d/charts/seasonal/forecast/eurosip/

II.4. IMPACT : PRECIPITATION FORECAST

There is a large contribution of the El Nino event to the forecasted anomalies distribution. Enhanced probability of excess precipitation in central and eastern equatorial Pacific extending to the coasts of Peru and Ecuador, and northward to Mexico and South of USA. The same in southern Brazil, Uruguay, and northern Argentina. Also on the Horn of Africa, the Great Lakes region and much of the Indian Ocean. Also enhanced probability of excess precipitation in Central Asia and China, and even very strong over eastern China, the Koreas and Japan.

Conversely, dry anomaly is expected on the Caribbean and northern South America, as well as southern Africa. A rainfall deficit is also very likely from the Maritime Continent up to Polynesia.

For Europe, a north-south gradient in the forecast seems to appear with an enhanced probability of dry anomaly on North Africa and the Mediterranean Sea and an enhanced probability of wet anomaly in the northwest of Europe. The boundary between these two areas is blurred and varies from one model to another. However the most probable signal is a wet signal over continental Europe.

II.4.a ECMWF

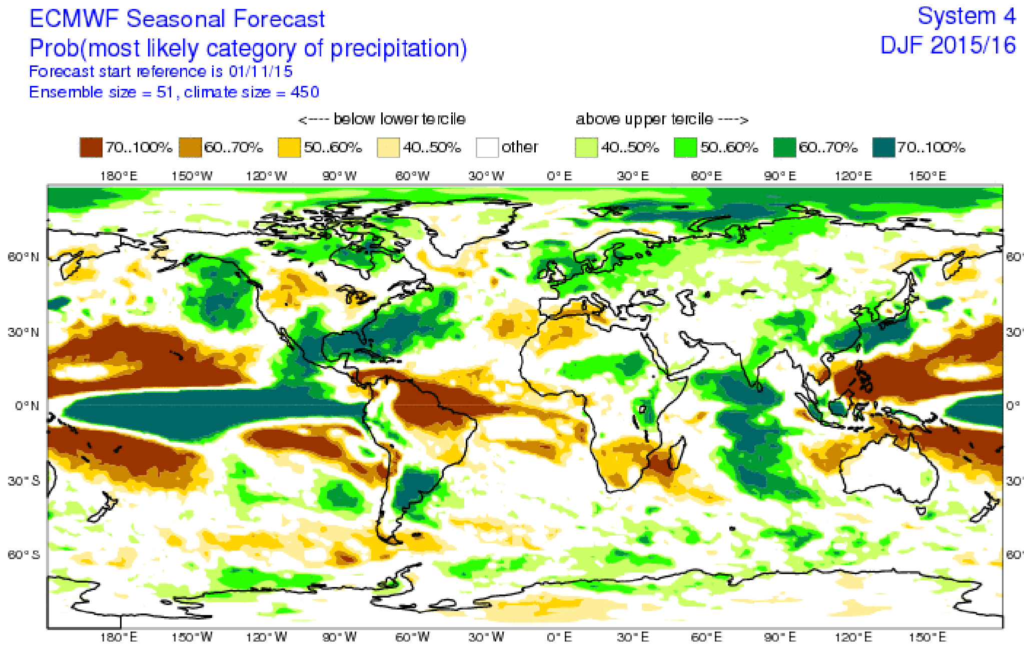

fig.II.4.1: Most likely category probability of rainfall from ECMWF. Categories are Above Normal, Below Normal and « other » category (Normal and No Signal). http://www.ecmwf.int/products/forecasts/d/charts/seasonal/forecast/

II.4.b Météo-France

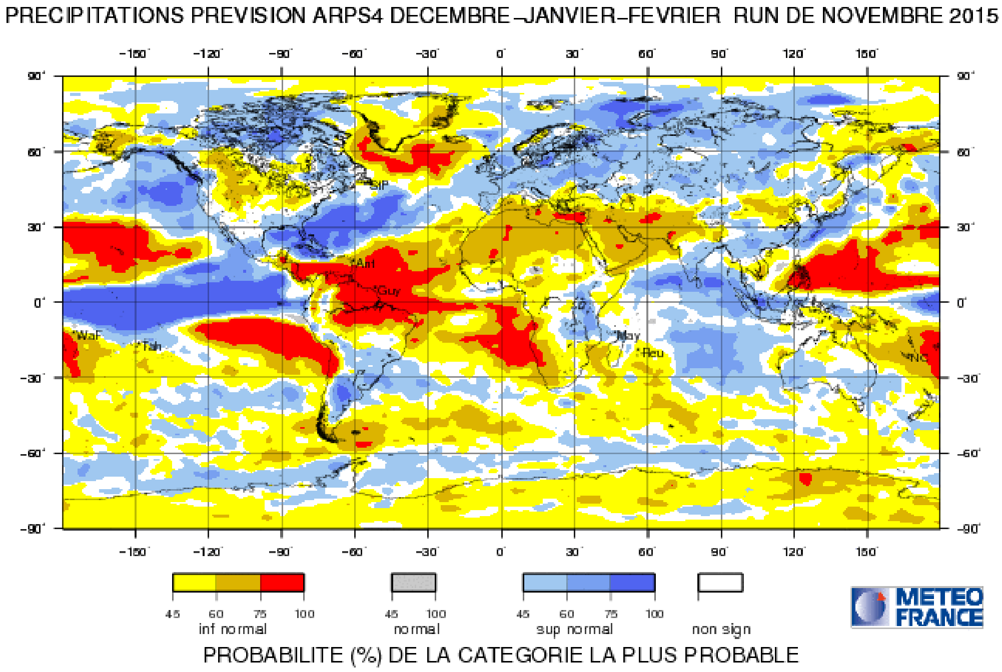

fig.II.4.2: Most likely category of Rainfall. Categories are Above, Below and Close to Normal. White zones correspond to No Signal. http://elaboration.seasonal.meteo.fr/

II.4.c Japan Meteorological Agency (JMA)

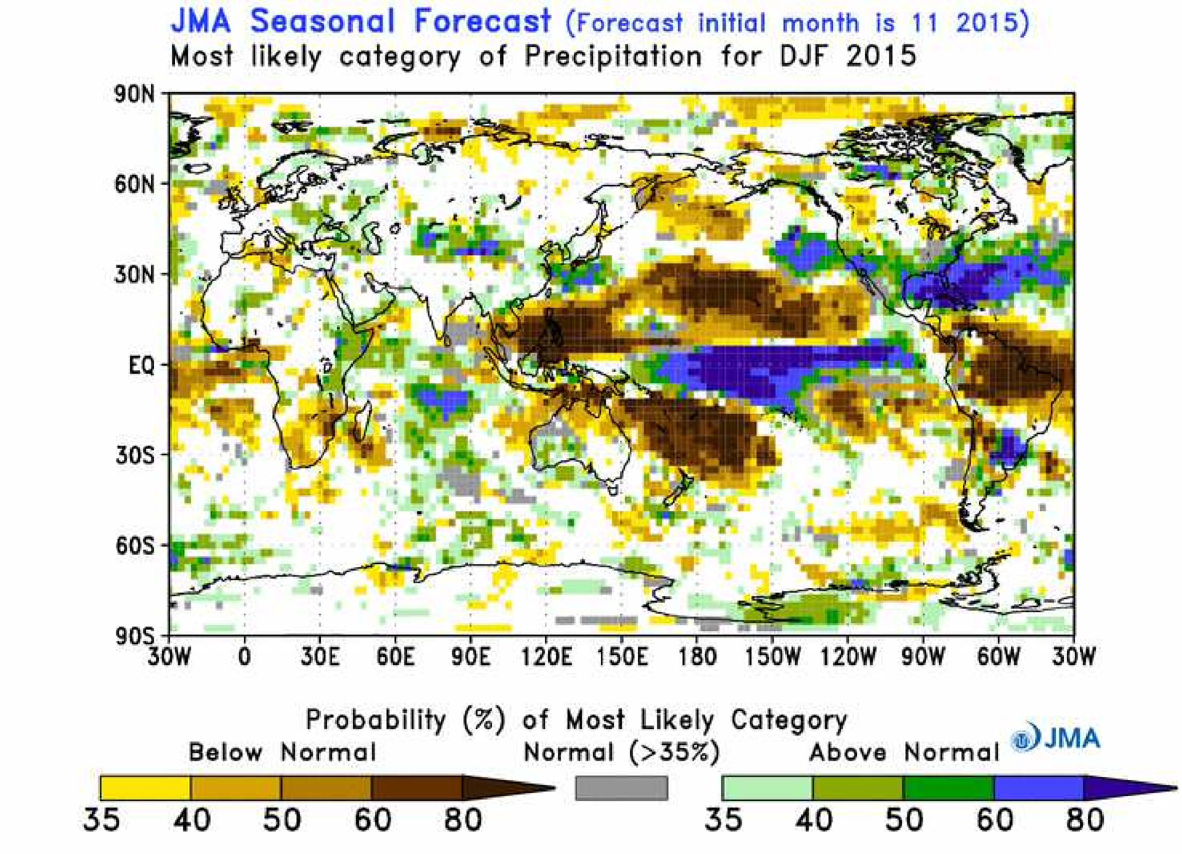

fig.II.4.5: Most likely category of Rainfall from JMA. Categories are Above, Below and Close to Normal. White zones correspond to No Signal. http://ds.data.jma.go.jp/tcc/tcc/products/model/probfcst/4mE/fcst/fcst_gl.php

II.4.d EUROSIP

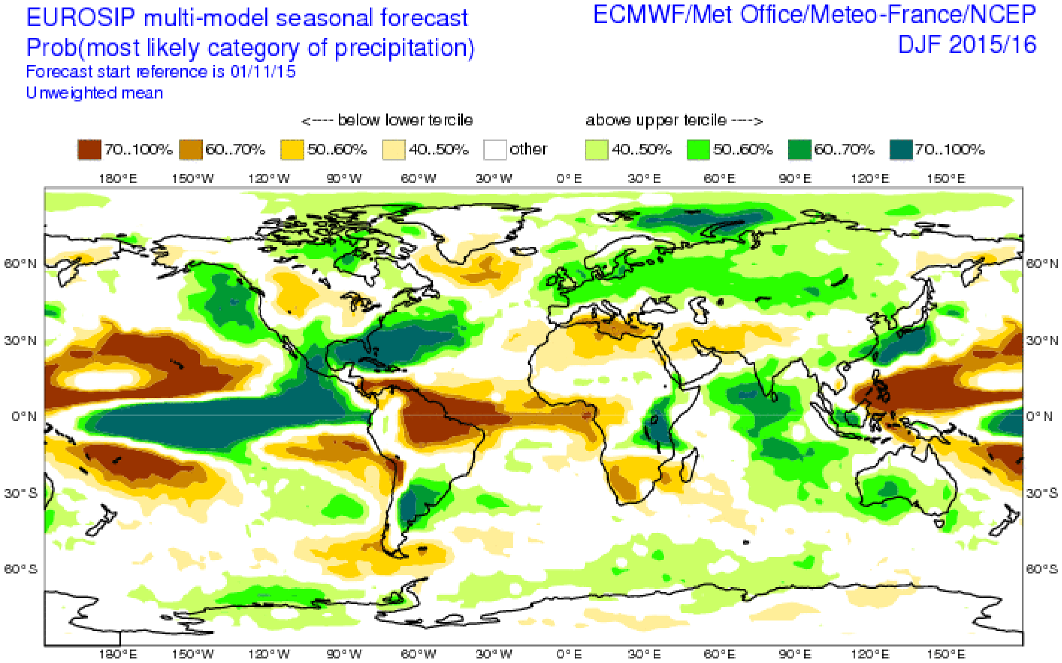

fig.II.4.7: Multi-Model Probabilistic forecasts for precipitation from EUROSIP (2 Categories, Below and Above normal – White zones correspond to No signal).

http://www.ecmwf.int/products/forecasts/d/charts/seasonal/forecast/eurosip/

II.5. REGIONAL TEMPERATURES and PRECIPITATIONS

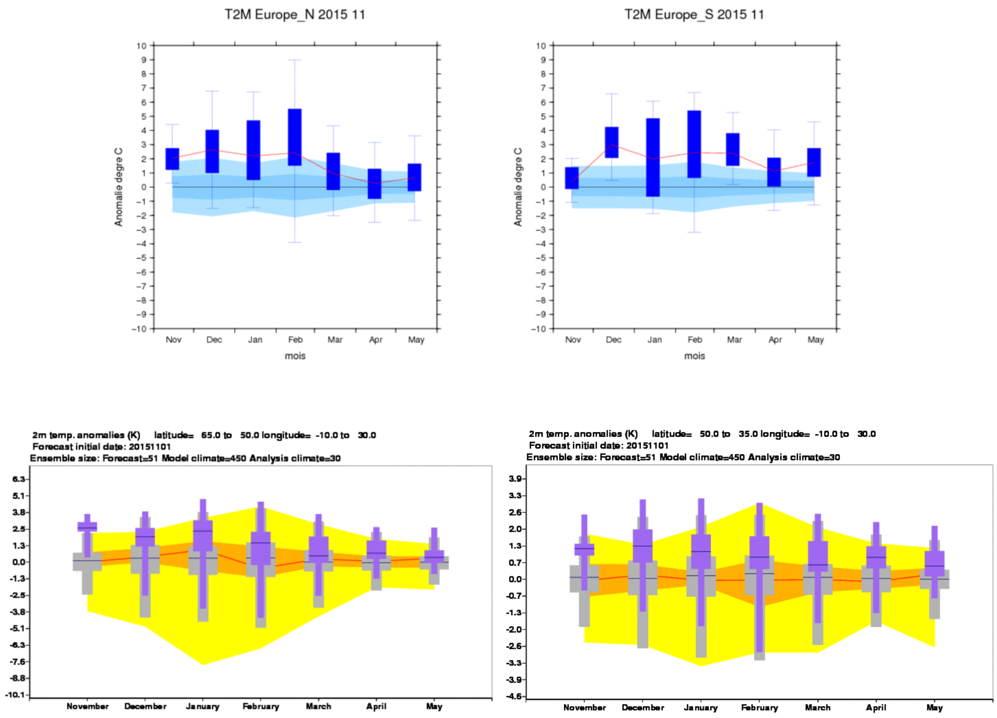

fig.II.5.1 : Climagrams for Temperature in Northern Europe (left) and in Southern Europe (right) from Météo-France (top) and ECMWF (bottom).

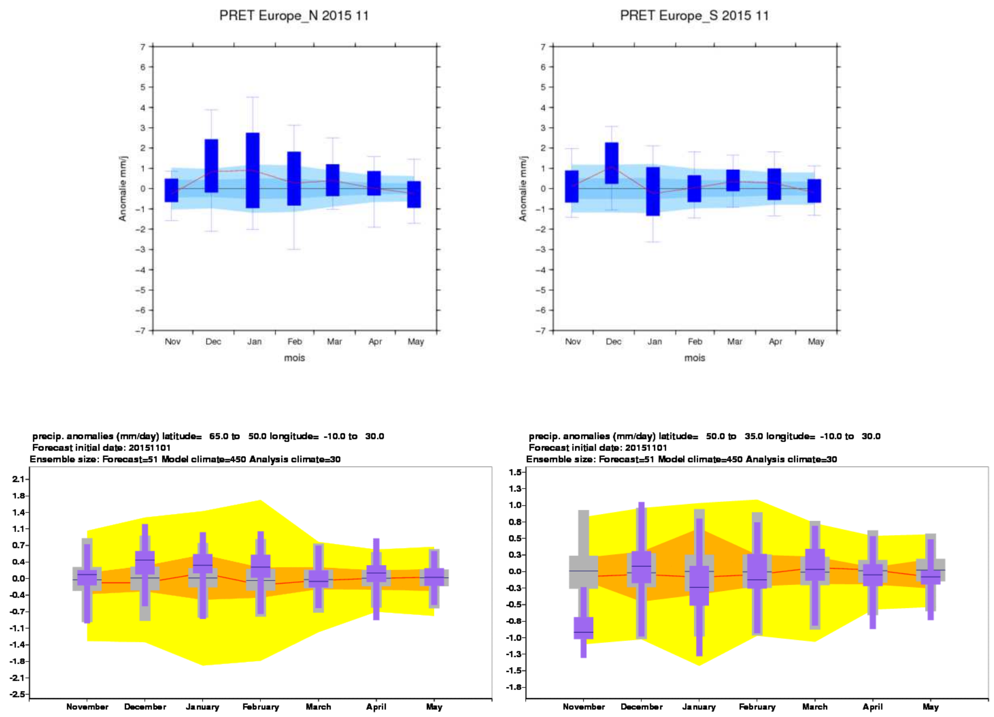

fig.II.5.2 : Climagrams for Rainfall in Northern Europe (left) and in Southern Europe (right) from Météo-France (top) and ECMWF (bottom).

II.6. MODEL'S CONSISTENCY

Not available

fig.II.6.1 : GPCs Consistency maps from LC-MME http://www.wmolc.org/

For SST :

For Z500 :

For T2m :

For Precipitation :

II.7. "EXTREME" SCENARIOS

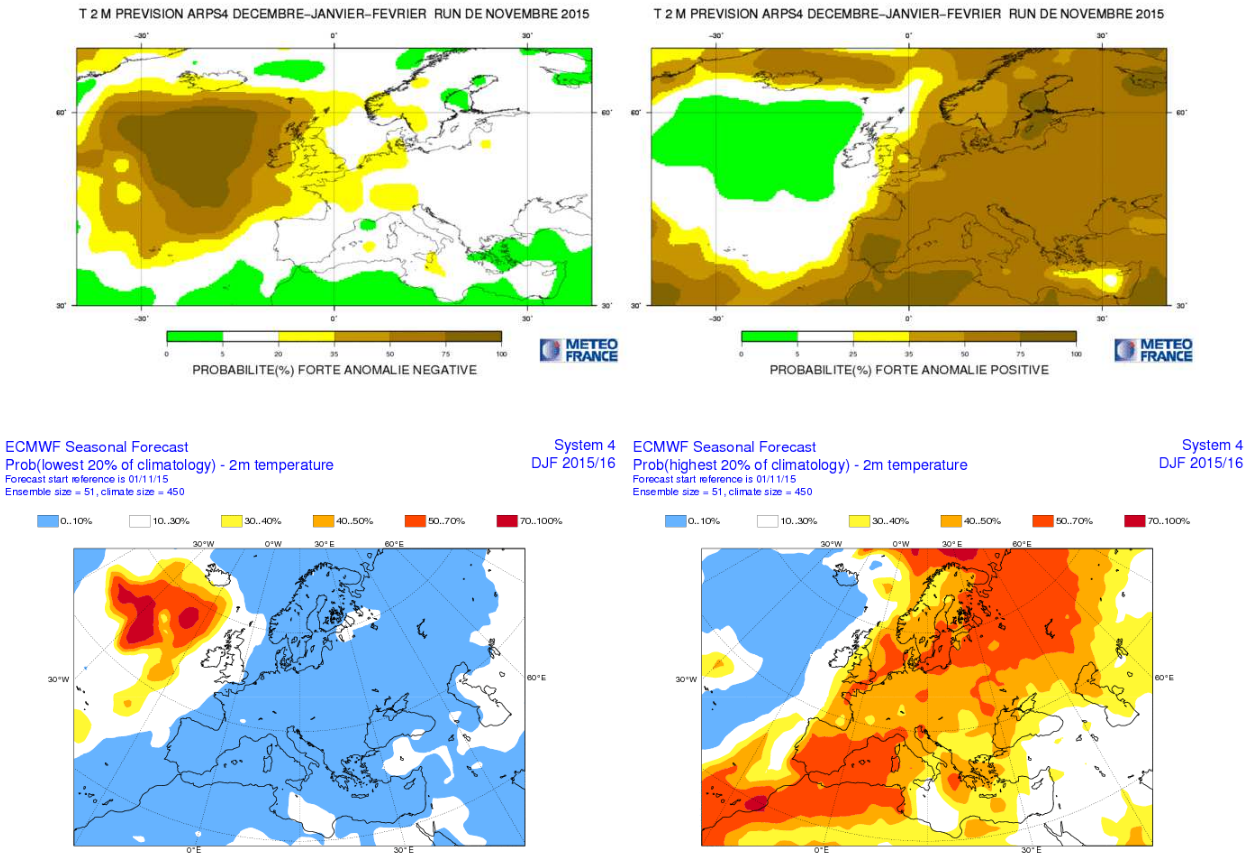

fig.II.7.1 : Top : Meteo-France T2m probability of « extreme » below normal conditions (left - lowest ~15% of the distribution) and "extreme" above normal conditions (right - highest ~15% of the distribution). Bottom : ECMWF T2m probability of « extreme » below normal conditions (left - lowest ~20% of the distribution) and "extreme" above normal conditions (right – highest ~20% of the distribution).

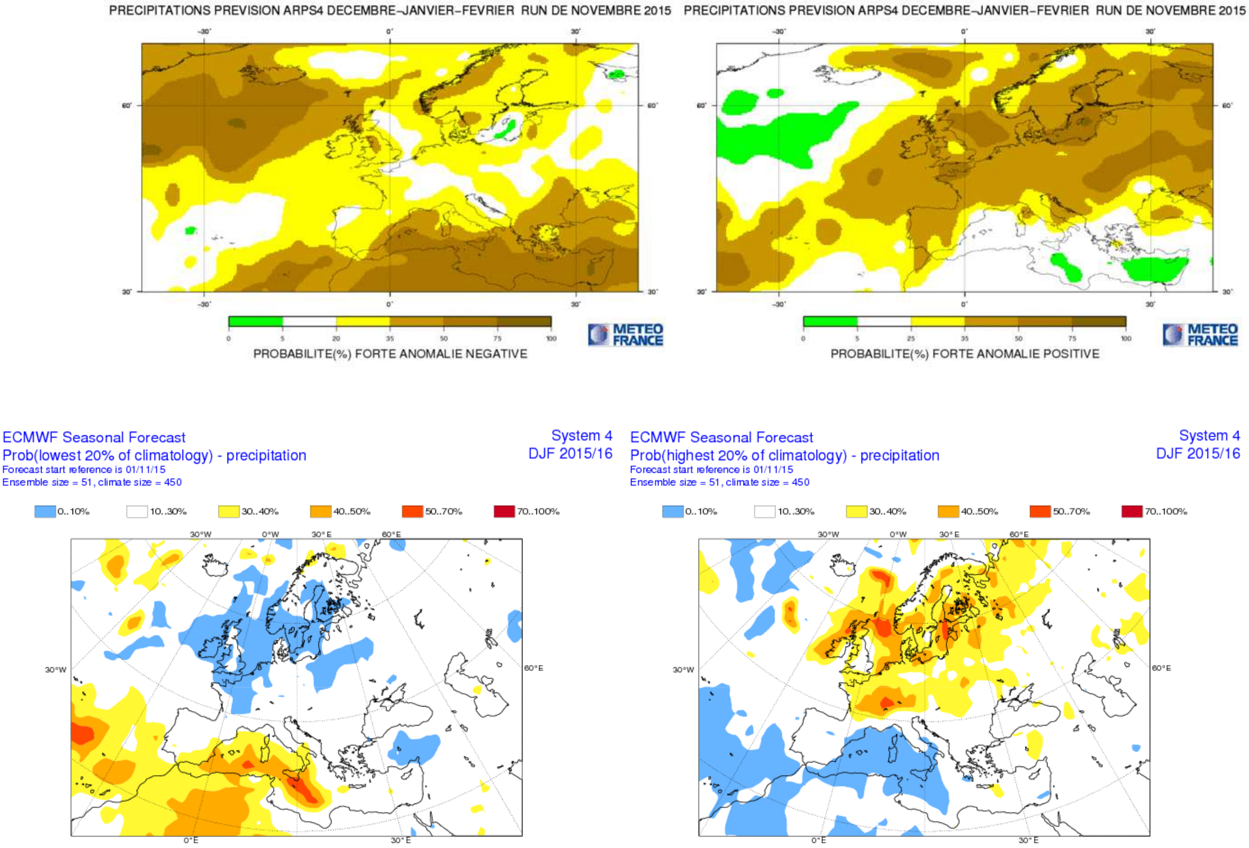

fig.II.7.2 : Top : Meteo-France rainfall probability of « extreme » below normal conditions (left - lowest ~15% of the distribution) and "extreme" above normal conditions (right - highest ~15% of the distribution).
Bottom : ECMWF rainfall probability of « extreme » below normal conditions (left - lowest ~20% of the distribution) and "extreme" above normal conditions (right – highest ~20% of the distribution).

II.8. DISCUSSION AND SUMMARY

II.8.a Forecast over Europe

Temperatures: More warmly than the normal signal on Europe, except British Isles where normal temperatures are likely.

Precipitation: wet signal (with higher probabilities in Northern Europe), dry signal over the Mediterranean Sea

Prévisions saisonnières probabilistes de températures pour le trimestre prochain

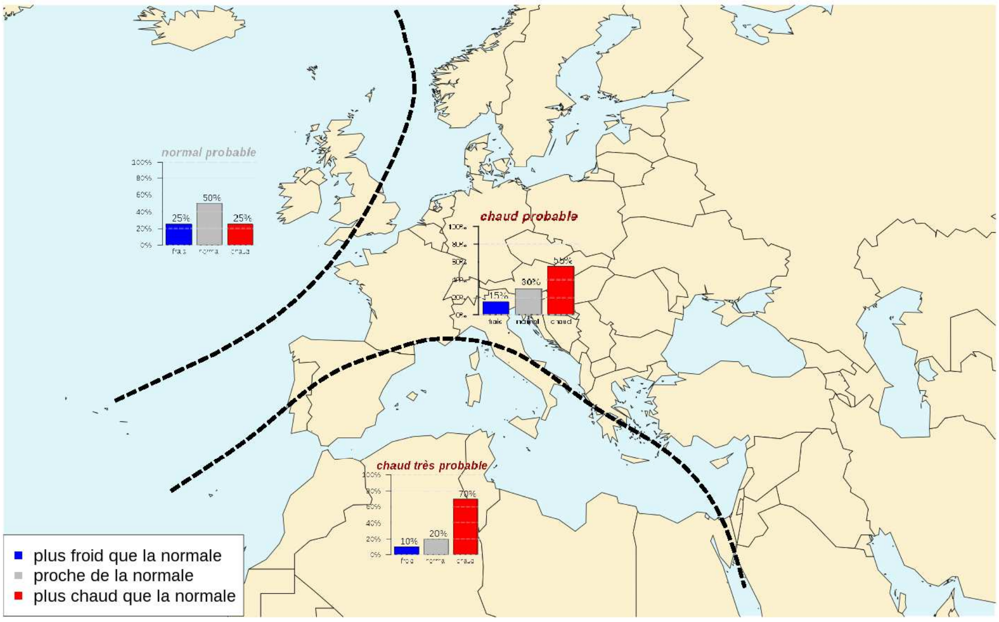

Prévisions saisonnières probabilistes de précipitations pour le trimestre prochain

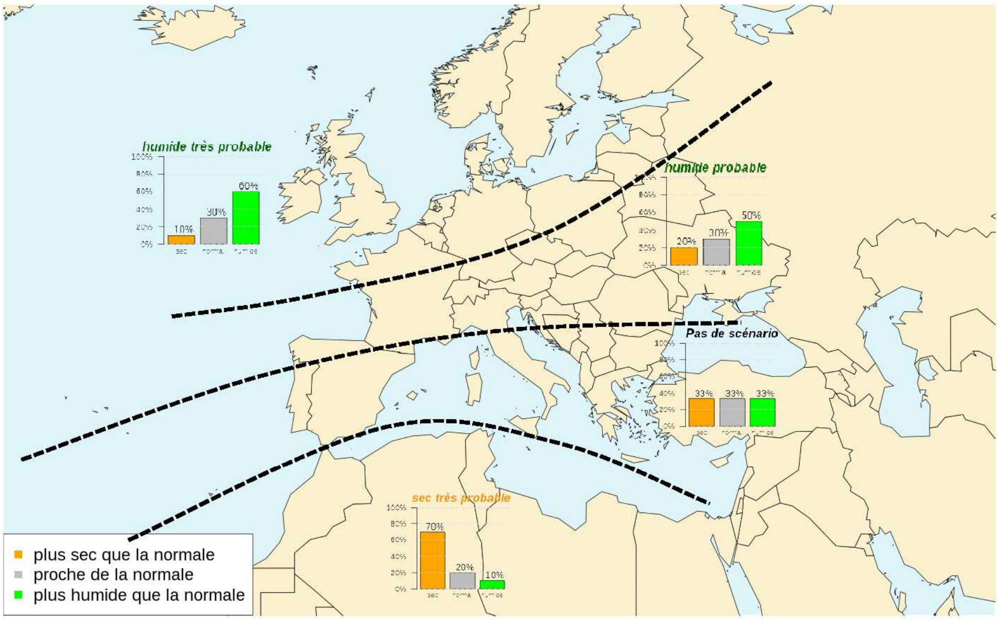

II.8.b Tropical cyclone activity

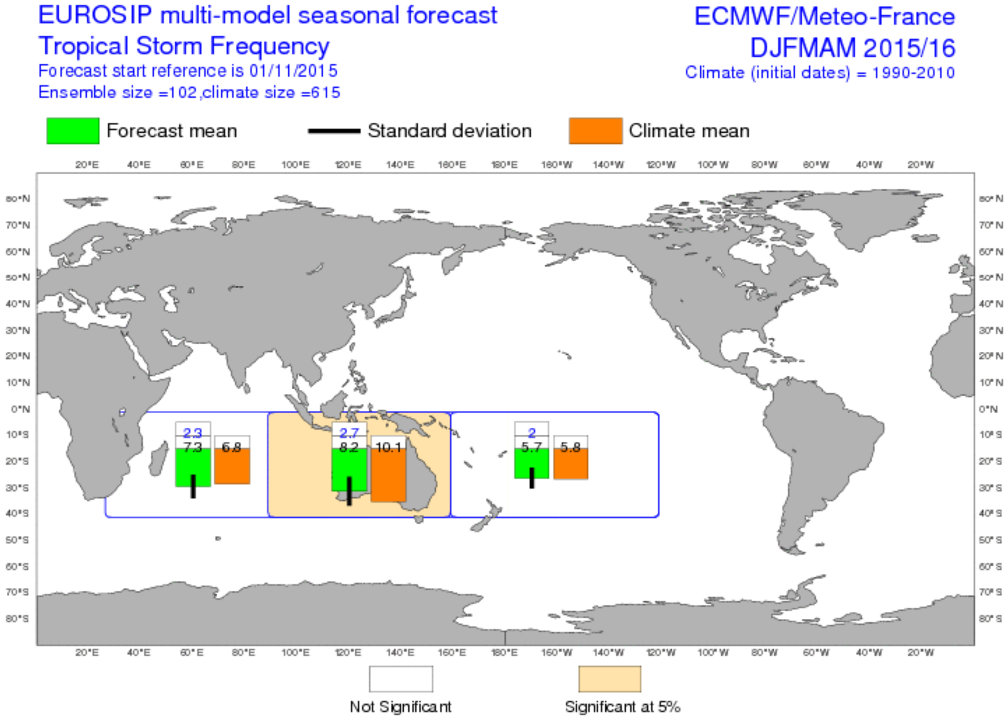

fig.II.8.1: Seasonal forecast of the frequency of Tropical Cyclones from EUROSIP (Météo-France & ECMWF).
http://www.ecmwf.int/products/forecasts/d/charts/seasonal/forecast/eurosip/

The hurricane season is expected lower than normal in the southwestern Indian Ocean (source : Meteo-France La Réunion) and significantly weaker in the southeastern Indian Ocean Indian Ocean (see EUROSIP). In south Pacific, the hurricane season is expected stronger than normal in the Polynesian area and weaker than normal in the southwestern Pacific so the mean over the EUROSIP box is not significant and does not reflect the impact of a strong El Niño.

ANNEX

II.9. SEASONAL FORECASTS

Presently several centres provide seasonal forecasts, especially those designated as Global Producing Centres by WMO (see http://www.wmo.int/pages/prog/wcp/wcasp/clips/producers_forecasts.html).

■ BoM, CMA, CPTEC, ECMWF, JMA, KMA, Météo-France, NCEP and UK Met Office have ocean/atmosphere coupled models. The other centres have atmospheric models which are forced by a SST evolution which is prescribed for the entire period of forecast.

■ LC-MME and Euro-SIP provide multi-model forecasts. Euro-Sip is presently composed using 4 models (ECMWF, Météo-France, NCEP and UK Met Office). LC-MME uses information coming from most of the GPCs ; providing deterministic and probabilistic combinations of several coupled and forced models.

Seasonal forecasts use the ensemble technique to sample uncertainty sources inherent to these forecasts. Several Atmospheric and/or oceanic initial states are used to perform several forecasts with slightly different initial state in order to sample the uncertainty related to imperfect knowledge of the initial state of the climate system. When possible, the model uncertainty is sampled using several models or several version of the same model. The horizontal resolution of the Global models is currently between 100 and 300km. This mean that only Large Scale feature make sense in the interpretation of the issued forecasts. Generally speaking, the temperature forecasts show better skills than rainfall forecasts. Then, it exists a natural weakness of the seasonal predictability in Spring (ref to North Hemisphere).

In order to better interpretate the results, it is recommended to look to verification maps and graphs which give some insight into the expected level of skill for a specific parameter, region and period. A set of scores is presented on the web-site of the Lead-Centre for Verification (see http://www.bom.gov.au/wmo/lrfvs/) ; scores are also available at the specific web site of each centres.

This bulletin collects all the information available the 21st of the current month preceding the forecasted 3-month period.

II.10. « NINO », SOI INDICES AND OCEANIC BOXES

El Niño and La Niña events primarily affect tropical regions and are monitored by following the SST evolution in specific area of the equatorial Pacific.

- Niño 1+2 : 0°/10°S 80W-90W ; it is the region where the SST warming is developing first at the surface (especially for coastal events).
- Niño 3 : 5°S/5°N 90W-150W ; it is the region where the interanual variability of SST is the greatest.
- Niño 4 : 5°S/5°N 160E- 150 W ; it is the region where SST evolution have the strongest relationship with evolution of convection over the equatorial Pacific.
- Niño 3.4 : 5°S/5°N 120W-170W ; it is a compromise between Niño 3 and Niño 4 boxes (SST variability and Rainfall impact).

Associated to the oceanic « El Niño / La Niña » events, and taking into account the strong ocean/atmopshere coupling, the atmosphere shows also interanual variability associated to these events. It is monitored using the SOI (Southern Oscillation Index). This indice is calculated using standardized sea level pressure at Tahiti minus standardized sea level pressure at Darwin (see above figure). It represents the Walker (zonal) circulation and its modifications. Its sign is opposite to the SST anomaly meaning that when the SST is warmer (respectively colder) than normal (Niño respectively Niña event), the zonal circulation is weakened (respectively strengthened).

Oceanic boxes used in this bulletin :

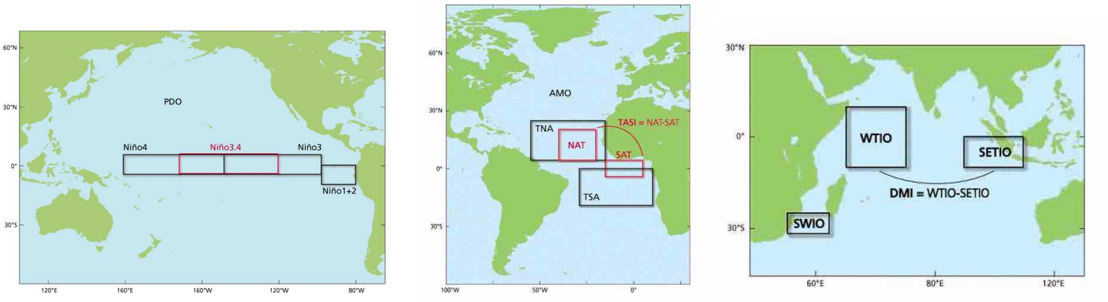

II.11.LAND BOXES

Some forecasts correspond to box averaged values for some specific area over continental regions. These boxes are described in the following map and are common to ECMWF and Météo-France.

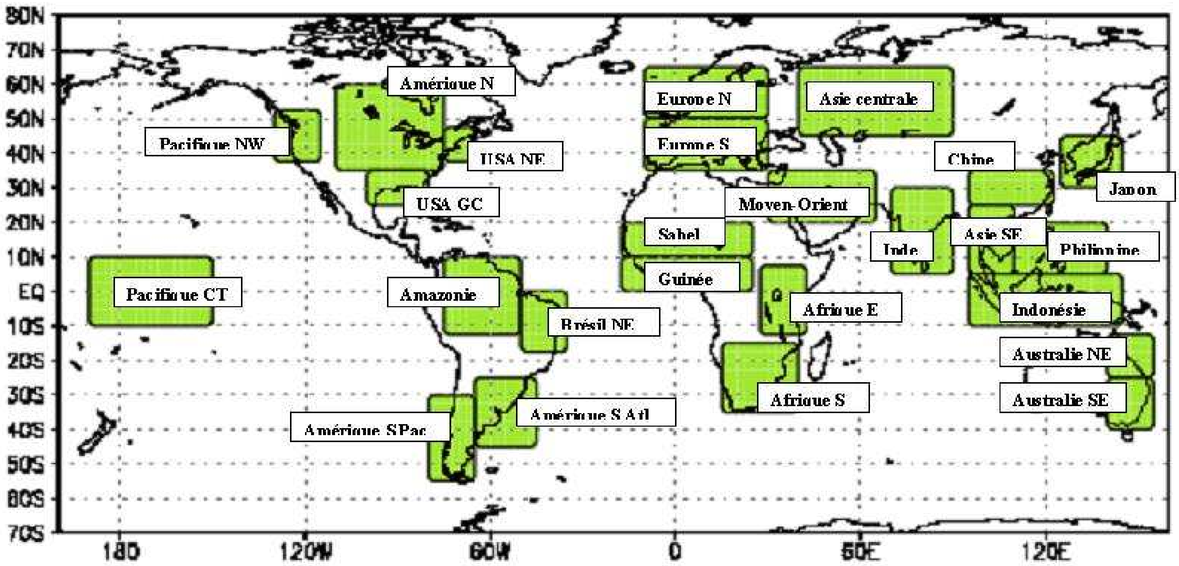

II.12. ACKNOWLEDGEMENT

This bulletin is edited by the RCC-LRF Node of the RCC Network in Toulouse for the RA VI. It is a joint effort of the RCC-Climate Monitoring Node (led by DWD) and the RCC-LRF Node (Co-Led by Météo-France).